Author:
Strauss, Amber A I

Title:
Assembly and characterisation of Diels-Alderase polymer conjugates for industrial biocatalysis

Author:
Strauss, Amber A I

Title:
ASSEMBLY AND CHARACTERISATION OF DIELS-ALDERASE POLYMER CONJUGATES FOR INDUSTRIAL BIOCATALYSIS

University of BRISTOL

ASSEMBLY AND CHARACTERISATION OF DIELS-ALDERASE POLYMER CONJUGATES FOR INDUSTRIAL BIOCATALYSIS

Name: Amber Strauss

School: Biochemistry

Supervisors: Dr. Paul Race and Dr. Steven Burston

Project type: Research master's

Start date: 01/10/17

This project is my own work except where indicated. All text, figures, tables, data or results, which are not my own work, are indicated and the sources acknowledged. In addition, I confirm that the hardcopy and the e-submission are identical.

Signed: _[redacted]_ Dated: 01/08/19

Abstract

The Diels-Alder reaction is a keystone reaction in synthetic chemistry. It is used extensively in the preparation of pharmaceuticals, crop protection agents and commodity chemicals. Diels-Alder biocatalysts offer expedient, green routes to a vast array of useful molecules, however, the development of industrially relevant Diels-Alderases has been hampered by their unsuitability for use at extremes of temperature, pressure and pH and their incompatibility with organic solvents. In this study a two-step polymer surfactant conjugation method has been developed, optimised and applied to the natural Diels-Alderase AbyU. This method involves the modification of protein surfaces through chemical super-charging, followed by polymer surfactant conjugation to form an amphipathic surfactant corona. The resulting AbyU-polymer conjugates exhibit increased tolerance to 'harsh' reaction conditions and enhanced catalytic efficiency versus the wild type enzyme. These data support the value of the outlined conjugation approach as a general method for improving biocatalyst tolerance to, and performance under, 'harsh' reaction conditions.

TABLE OF CONTENTS

List of Abbreviations

[C-AbyU] – Cationised AbyU

[C-AbyU][S] – Surfactant Conjugated AbyU

[N-AbyU] – Native AbyU

BSA – Bovine Serum Albumin

CD – Circular Dichroism

EDC – 1-ethyl-3-(-3-dimethylaminopropyl) carbodiimide hydrochloride

DMPA – N,N-dimethyl, 1-,3-propendiamine

GuHCl – Guanidium Hydrochloride

LB – Lysogeny Broth

LC-MS – Liquid Chromatography coupled Mass Spectrometry

MALDI-MS – Matrix-Assisted Laser Desorption Ionization-Mass Spectrometry

Ni – Nickel

Ni-NTA – Nickel-Nitrilotriacetic Acid

SAXS – Small Angle X-ray Scattering

SEC – Size Exclusion Chromatography

Tm – Melting temperature

List of Figures

List of Tables

Chapter 1. Introduction

An important part of the drive towards environmentally friendly, green chemical synthesis is a reduction in the use of synthetic catalysts, and their substitution with enzymes (Turner & Truppo, 2013). Enzyme-based biocatalytic processes offer a highly selective, safe, and sustainable route to the scalable production of a multitude of important molecules (Truppo, 2017). Unlike many chemical catalysts, biocatalysts often exhibit exquisite enantio- and stereoselective control of the reactions that they perform, offering expedient routes to the assembly of complex molecules that present a challenge to conventional synthetic methodology (Choi, Han, & Kim, 2015). Through protein engineering, enzymes can be modified to change their properties, for example to enable the selection and transformation of 'non-natural' substrates, or to make them compatible with specific industrial processes or reaction conditions (Renata, Wang, & Arnold, 2015). Furthermore, enzymes are produced from low cost renewables, and are inherently biodegradable. Enzymes therefore offer an efficient means to produce a homogenous pool of active molecules, through iterative rounds of reaction cycles before degradation (de Regil & Sandoval, 2013). Biocatalysts that perform carbon-carbon bond forming reactions are particularly highly sought after, as they enable atom-efficient, enantioselective assembly of complex organic scaffolds to produce active versions of important compounds such as pharmaceuticals, crop protection agents and commodity chemicals (Schmidt, Eger, & Kroutil, 2016).

The need for powerful biocatalysts is exemplified in the pharmaceutical industry. The demand for new antibiotics has become a pressing problem in recent years. Antibiotics have revolutionised modern medicine, however, resistance acquisition continues to outpace antibiotic development (SMAC, 1998). Resistance selection is an inevitable consequence of antibiotic use, therefore the development for new antibiotics with diverse, or ideally new, modes of action is urgently needed. Natural products represent a leading source for drug candidates, especially antibacterial agents (Dias, Urban, & Roessner, 2012). For example, pioneering research in the 1940s into the anti-bacterial mechanisms of microbes, led to the discovery of streptomycin (Hughes & Karlén, 2014). Currently, research has also explored the production of new drugs from the metabolites of microbes (Ruiz, et al., 2010), through the

refinement of natural enzymes that have evolved to produce them. Therefore, modifying natural enzymes, for example through directed evolution or genetic approaches, represents a promising method for enabling access to new antibiotics, *via* the production of 'non-natural' natural products (Chandra Mohanaa, et al., 2018).

Microorganisms which exist under extreme environmental conditions are likely to yield unique and powerful bioactive compounds, to which resistance has not yet emerged (Subramani & Aalbersberg, 2012). It is posited that exposure to such 'extreme' conditions drives the acquisition of metabolic innovations, which in turn translates into the production of novel bioactive natural products. *Verrucosispora maris,* a deep-sea bacterium which lives on the Pacific seabed (Goodfellow, et al., 2012), produces a family of polycyclic antibiotics which include abyssomicin C (Figure 1.1). Enzymes involved in the biosynthesis of this compound are the focus of the research outlined in this thesis. Abyssomicin C shows antibiotic activity against Gram-positive bacteria including pathogenic strains of methicillin resistant *Staphylococcus aureus* (MRSA) (Riedlinger, et al., 2004). It has a unique mode of action, targeting the bacterial folate biosynthesis pathway, the product of which is required for DNA processing and maintenance. This pathway is absent in humans, minimising the possibility of off target effects and improving the likelihood of clinical viability.

Abyssomicin C is biosynthesised by a Type I modular polyketide synthase (PKS) pathway (Figure 1.1). Polyketides are a functionally diverse class of molecules bearing clinically relevant pharmacological activities, for example the anticancer agent Epothilone (Osswald, et al., 2014) and the antibiotic Erythromicin (Vieweg, Reichau, Schobert, Leadlay, & Süssmuth, 2014). The enzyme AbyU acts during the later stages of abyssomicin C biosynthesis, where it catalyses an enantiomerically-selective formal Diels-Alder reaction to yield a spirocyclic product from a linear polyketide substrate (Byrne, et al., 2016). It has been proposed that modification of AbyU could offer a route to the production of functionally optimised abyssologues, with improved clinical performance as compared to the native natural product. Significantly, this work unlocks a wealth of options for making new bioactive compounds that could form the basis of new therapeutics, materials, and platform chemicals, amongst others.

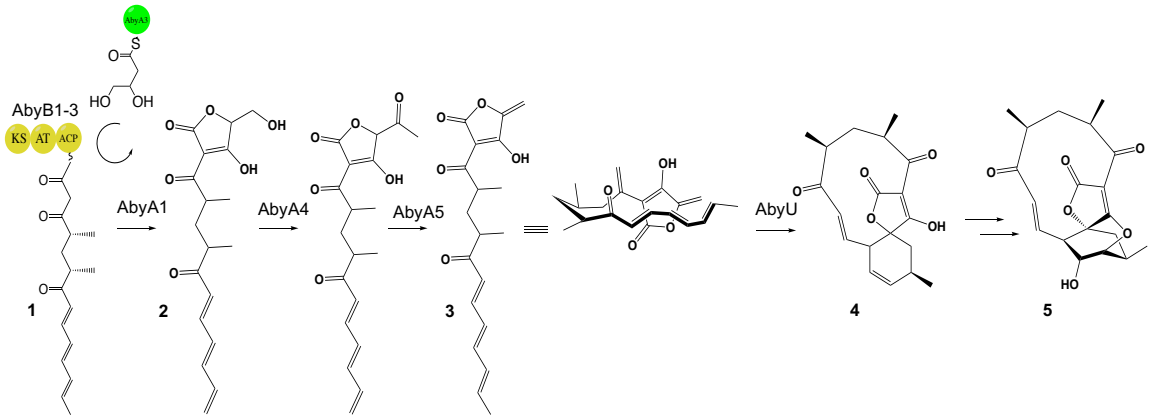

Figure 1.1 Proposed abyssomicin C biosynthetic pathway. The multi-modular PKS complex (AbyB1-3) biosynthesises a linear polyketide product, which is coupled to an ACP-tethered C3 precursor, which originates from 1,3-bisphosphoglycerate. The linear polyketide **1**, is condensed with the C3 unit covalently attached to the free-standing thiolation domain AbyA3 to form the five-membered tetronate ring of **2**. This compound is subsequently acetylated by AbyA4, followed by an AbyA5 catalysed acetate elimination. These steps install the distinctive exocyclic methylene group of **3**. An enzyme catalysed intramolecular Diels–Alder, performed by the enzyme AbyU, then takes place between the exocyclic methylene of 3 and a diene present in the conjugated triene system of **3**, generating the spirotetronate nucleus of atrop-abyssomicin C in **4**. Tailoring macrocyclic **4** gives abyssomicin C (**5**) and related compounds. Adapted from (Byrne, et al., 2016).

1.1 The Diels-Alder Reaction

In a Diels-Alder reaction, an unsaturated hydrocarbon containing two C=C bonds (the diene), reacts with a dienophile, which is usually an electron-poor alkene group or alkyne group (Figure 1.2). This is an example of a [4+2] cycloaddition, in which one reactant molecule contributes four π electrons and the other two π electrons to yield a [4+2] cycloadduct.

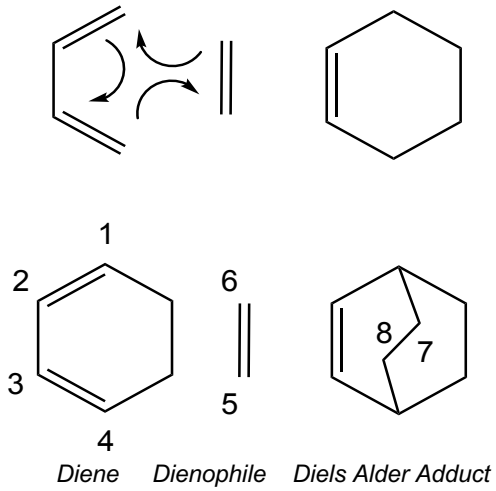

Bonds formed	Bonds broken
$C_1 – C_6$	$C_1 – C_2$ (π)
$C_2 – C_3$ (π)	$C_3 – C_4$ (π)
$C_4 – C_5$	$C_5 – C_6$ (π)

Figure 1.2 The Diels-Alder reaction. Adapted from *Cyclic Dienes and Dienophiles in the Diels-Alder Reaction* (Chemistry, 2018). Black curly arrows represent the movement of electrons.

The Diels-Alder reaction is thermally sensitive. Heat will favour the forward reaction, whilst high heat will favour thermal decomposition of the covalent bonds formed between the diene and dienophile, through the retro-Diels–Alder reaction (Liu, Hsieh, & Chen, 2006). Diels-Alder reactions also respond to adjustments in pressure, allowing many factors to be optimised to increase yield. A major obstacle for the use of biocatalysts in organic synthesis is their thermodynamic and kinetic instability under harsh reaction conditions. Since industrial processes often involve high temperature reactions and extreme pressure, modification of enzymes to confer improved tolerance to these conditions is invaluable.

1.2 Structure of the Natural Diels-Alderase AbyU

The abyssomicin C precursor is a macrocyclic spirotetronate, which comprises a tetronic acid ring spiro-linked to cyclohexene. This compound has recently been shown to be produced by a Diels-Alder reaction, catalysed by the enzyme AbyU (Byrne, et al., 2016). The AbyU core adopts a distinctive β-barrel fold. A flexible loop (residues Asp26-Gly36 between sheets β1 and β2) is believed to regulate entry and exit of the enzyme's active site cavity (Figure 1.3). Based on molecular modelling studies of the enzyme in complex with its substrate, the majority of interactions between residues in the enzyme active site and the cognate AbyU substrate are hydrophobic in nature, with a solitary hydrogen bond predicted between a substrate carbonyl and the side chain of Tyr76 (Byrne, et al., 2016).

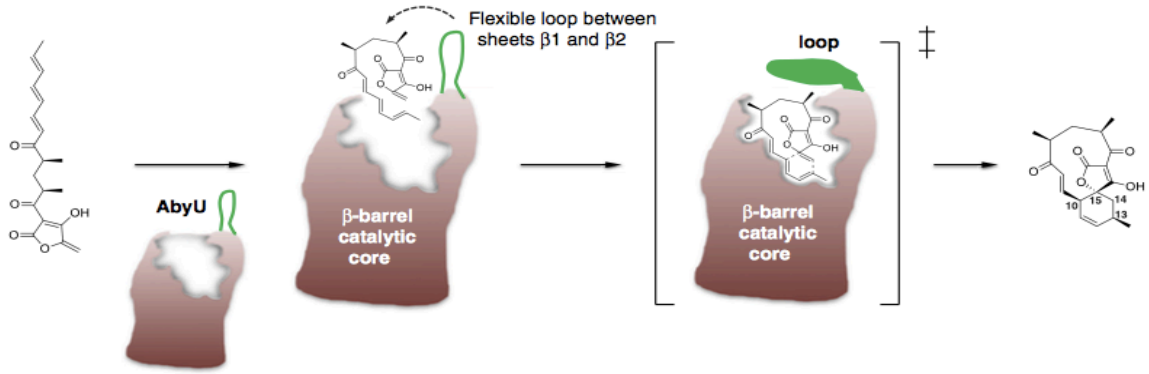

Figure 1.3 Schematic of the AbyU catalysed Diels-Alder reaction. (Hashimoto & Kuzuyama, 2016).

AbyU is a dimer in solution. The internal channel of each barrel monomer is book-ended by a salt bridge formed between the residues Glu19 and Arg122 and a predominantly hydrophobic loop which joins β1 to β2 (Figure 1.4). AbyU-catalysed bond formation (2x C-C bonds) occurs concerted, albeit asynchronous manner, *via* resolution of the energetically favourable transition state. The shape of the enzyme active site optimally matches that of the transition state of the reaction. This allows the bond formation to proceed with a low free-energy barrier (Byrne, et al., 2016).

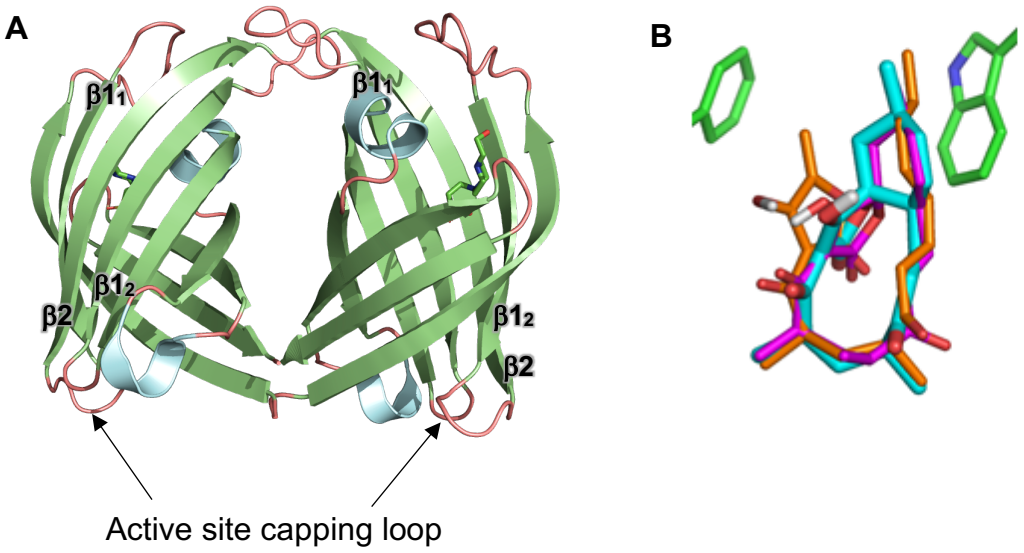

Figure 1.4 (A) Crystal structure of the AbyU dimer, coloured by 2° structure (β structure in green, α structure in blue and flexible loops in pink). The substrate mimic HEPES is observed in the enzyme active site and is shown in stick format. **(B)** Docking simulation of the conformation of the AbyU product (cyan carbons), overlaid with the equivalent poses of the docked substrate (orange carbons) and the intermediate product (magenta carbons) in the AbyU active site. Active site residues Phe41 and Trp124 are indicated for reference (green carbons). Adapted from Byrne, et al. 2016.

To date, nine gene clusters of spirotetronate antibiotics have been identified, all of which possess AbyU-like putative Diels-Alderases (Zheng, et al., 2016). In addition, the large number of natural products that contain [4+2] adducts suggests the existence of many more natural enzymes that can catalyse Diels-Alder reactions. In contrast to *de novo* designed Diels-Alderases, whose active sites are derived from computational models based on a set of existing protein scaffolds (Preiswerk, et al., 2014), and which can only act upon simple substrates, most natural [4+2] adducts have complex structures. Therefore, modification of natural Diels-Alderases is likely to provide a route to a multitude of increasingly complex bioactive chemical architectures. Conversely, naturally evolved Diels-Alder biocatalysts represent attractive frameworks for directed evolution to develop industrially relevant enzymes for this reaction.

1.3 Modification of AbyU

An obstacle to the utility of AbyU is that its substrate and product, although miscible in water, require organic solvents to help dispersion and prevent aggregation. This is a direct consequence of the distinctive C3 carbon tail present in the molecule. However, if the enzyme were modified appropriately, it could be active in a solvent-free state, making it much more useful in industrial applications. An example of such a modification is protein bioconjugation. Conjugation aims to chemically couple a biomolecule with other molecules to form stable conjugates, resulting in the combined properties of the constituent components or enhanced properties from synergistic effects (Hermanson, Bioconjugate techniques, 1996). Once assembled, these conjugates may be used for a broad variety of applications, for example therapeutics, imaging probes or as a catalytic system (Hermanson, PEGylation and Synthetic Polymer Modification, 2013). Several techniques are reported in the literature that involve crosslinker and modification reagents, and include, for example, PEGylation; the attachment of polyethylene glycol (PEG) to proteins. This can endow desirable attributes such as improved water solubility and thermal stability (Zalipsky, 1995). The bioconjugation methods employed in the work outlined in this thesis is a two-step protocol that involves cationisation, which introduces a positive charge to the protein surface, followed by surfactant conjugation and the attachment of a synthetic polymer to the outside of the charged protein. The enzyme can then be lyophilised and freeze-dried, allowing it to be taken it out of aqueous solution whilst retaining its function (Brogan, Sharma, Perriman, & Mann, 2013).

1.4 Cationisation

Enzyme cationisation is a well-established bio-conjugation technique in which the acidic amino acids aspartate and glutamate on the protein surface are bonded to amines, creating a positively charged cross-linked protein. To perform cationisation, a cross-linking agent that contains reactive termini able to attach to functional groups is often required (Farkaš & Bystrický, 2010). Potential functional groups include primary amines (–NH2), which are found at the N-termini of proteins, or carboxyl groups (–COOH), at the C-termini of polypeptide chains. Classical strategies employed in chemical coupling include; reductive amination, where free aldehydes (-CHO) and ketones (RC(=O)R') are reacted with amines; amide bond formation; and activation of hydroxyl (-OH) groups (Montalbetti & Falque, 2005). Preferential conjugation with amines represents one of the most used widely reactions to introduce linkers to biomolecules, and results in amide bond formation (Montalbetti & Falque, 2005). This requires a preparative step turning the carboxylic acid into an active ester. Carbodiimide-based activation of carboxyl groups, as employed in this study, is the most commonly used method for active ester preparation (Warhi & Al-Hazimi, 2012), with N-substituted carbodiimides widely used in bioconjugate chemistry, specifically 1-ethyl-3-(-3-dimethylaminopropyl) carbodiimide hydrochloride (EDC) (Grabarek & Gergely, 1990) (Figure 1.5). This agent forms active esters in a single step and was chosen to be used in this study due its compatibility with biomacromolecules including polypeptides (Extance, 2016).

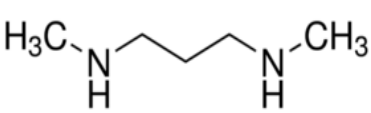

DMPA, 102.18 g.mol^{-1}

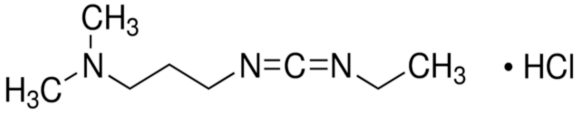

EDC, 191.7 g.mol^{-1}

Figure 1.5 Chemical structures of the cationising agents, N,N-dimethyl, 1-,3-propendiamine (DMPA) and EDC.

Cationisation has many advantages over alternative bioconjugation methods. Significantly, the addition of negatively charged compounds or particles through electrostatic interactions does not disrupt the quaternary structure of target proteins. Enzyme supercharging has already been shown to improve folding robustness and impart aggregation resistance, without abolishing enzyme function (Lawrence, Phillips, & Liu, 2007). For example, it has been extremely successful with other proteins, such as green fluorescent protein (GFP), as extensively mutating the surface of a protein to enhance their overall charge was seen to enhance thermodynamic stability (Strickler, et al., 2006). In this study cationisation is used to attach a negatively charged surfactant polymer to the protein AbyU, to enable the assembly of a sophisticated protein-based biomaterial (Armstrong, et al., 2015). Modification of protein surfaces is achieved by coupling of N,N-dimethyl, 1-,3-propendiamine (DMPA) to aspartate and glutamate side chains using EDC (Correia Carreira, 2017) (Figure 1.6). DMPA is added to the solution first, and the reaction is started with the presence of EDC in the solution. EDC covalently attaches to the protein and catalyses charge switching by activating the protein carboxyl groups. DMPA amidates the activated carboxylic acids, covering the protein surface in positive charge. This is highly pH dependent, since an acidic pH protonates amine groups of DMPA. Furthermore, the theoretically calculated isoelectric point of AbyU (based on amino acid composition) is pH 5.5, hence pH must be closely monitored to prevent protein precipitation. It has also been shown that EDC will coat the protein with 90% efficiency between pH's 4 and 6 (Mr. Carl Marsh, personal communication).

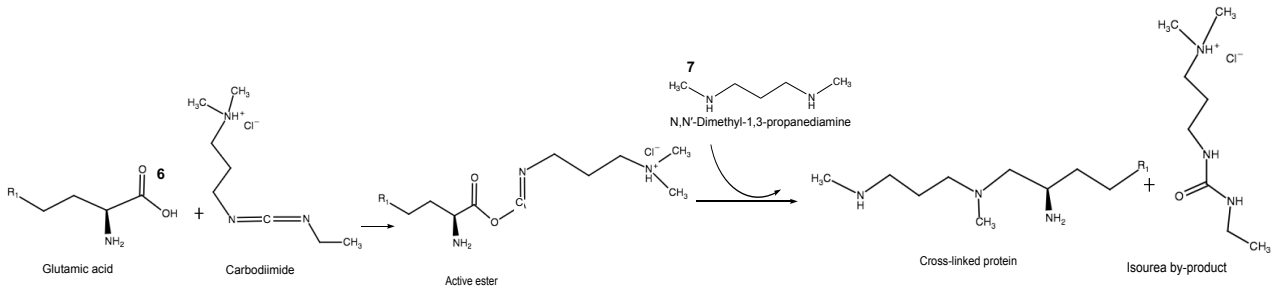

Figure 1. 6 Carboxyl-to-amine crosslinking involving the use EDC. Molecules **6** and **7** are required to have a carboxylate and an amine group respectively, for this reaction to occur.

In AbyU, the majority of the polar amino acids reside on the outside of the protein (Figure 1.7). This is important as it means cationisation is unlikely to affect the enzyme active site, and thus negatively impact the ability of the enzyme to catalyse the Diels-Alder reaction. It should be noted that changes in surface electrostatics resulting from supercharging could destabilise the protein structure, however, the total volume of the internal volume of the AbyU active site is limiting and is likely to cause too much steric hindrance as to allow the DMPA molecule to assume the correct geometry for attaching to the acidic residues within the active site. Therefore, techniques to study protein folding, such as circular dichroism (CD) spectroscopy, will need to be employed to make sure that these predictions are accurate.

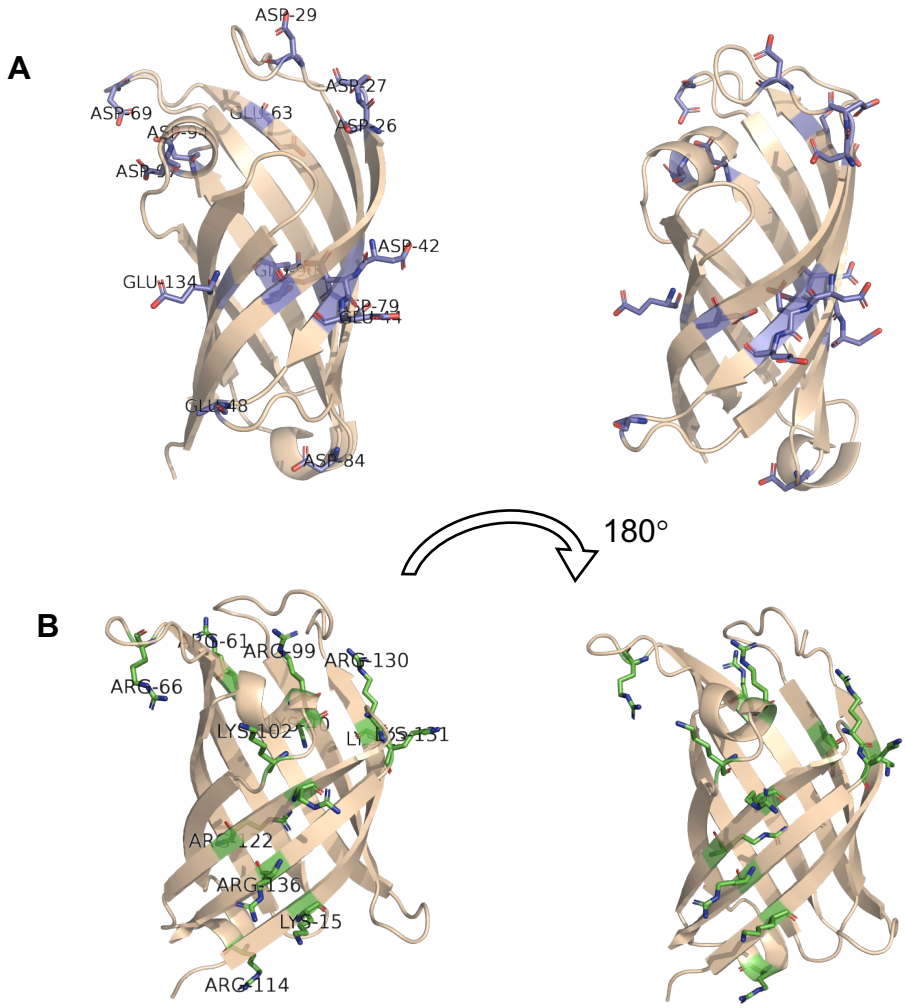

Figure 1.7 Structures of AbyU. (A) Negatively charged aspartic and glutamic acid residues in blue. **(B)** Positively charged external arginine and lysine residues in green.

1.5 Conjugation

The directed modification of polypeptides *via* bio-conjugation has proven a useful technique to improve natural systems and generate therapeutic protein constructs (Spicer & Davis, 2014). Here, conjugation describes the addition of the surfactant polymer IGEPAL-890, to the outer surface of the enzyme, AbyU, *via* electrostatic interactions forming a “corona” or outer shell (Figure 1.8). This particular reaction, using an anionic surfactant, has found considerable applications in organic synthesis, materials chemistry and for the bioconjugation of larger constructs (Brogan & Hallet, 2016). The polymer IGEPAL-890 was chosen due to its hydrophobic nonylphenyl tail, which has been shown to facilitate persistent membrane affinity (Armstrong, et al., 2015). This is desired, for example, to create a surface-functionalised Diels-Alder system or for extending the shelf life of AbyU by partitioning it into liposomes. The polyethylene oxide structure has also been shown to prevent protein denaturation, which is highly useful for application in industrial processes (Armstrong, et al., 2015). The primary alcohol (hydroxyl) group of the surfactant, IGEPAL-890 is oxidised and attracted to the positively charged amino acids on the external surface of the protein.

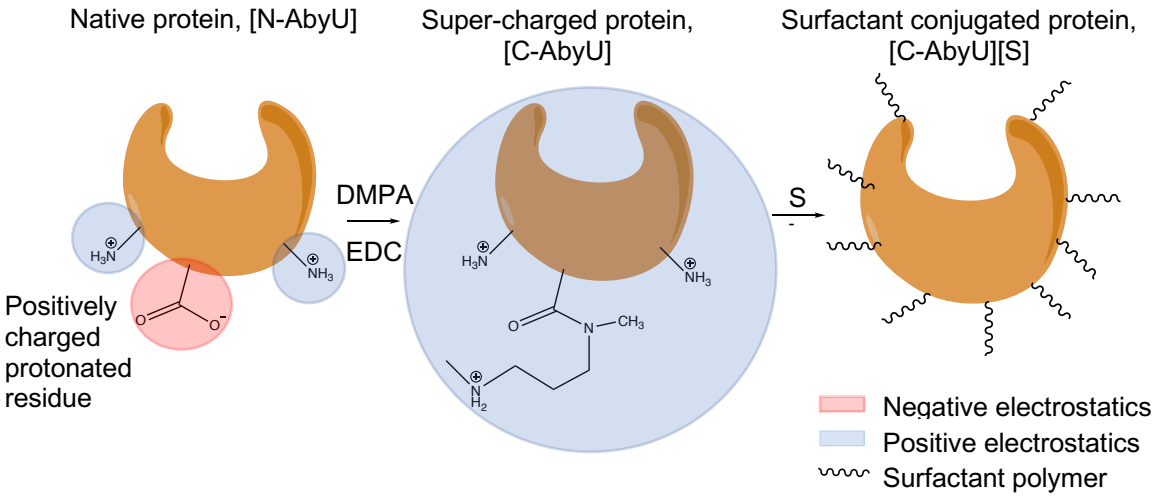

Figure 1.8 Carbodiimide-mediated cationisation of AbyU. A glutamic acid side-chain of native AbyU, [N-AbyU], is modified by N,N-dimethyl-1,3-propanediamine (DMPA) to yield cationised AbyU, [C-AbyU], followed by electrostatic coupling with oxidised surfactant (S^-), to give conjugated AbyU, [C-AbyU][S].

A reported effect of conjugation is that it improves enzyme stability, possibly by creating an outer-shell casing around the protein that imparts enhanced structural integrity (Armstrong, et al., 2015). Furthermore, bio-conjugation of proteins using cationisation and electrostatic binding of appropriately charged surfactant polymers has been shown to generate a dehydrated pure protein melt upon lyophilisation (Perriman, Cölfen, Hughes, Barrie, & Mann, 2009), These conjugates could be used, for example, to facilitate membrane insertion, to form membrane micro-bioreactors, which have wide applications in environmental treatment, pharmaceutical manufacture and energy generation (Chakraborty, et al., 2016). The choice of surfactant can direct which solvent an enzyme can be solubilised in. For example, to dissolve a protein into a polar solvent, such as acetonitrile, an amphipathic surfactant must be selected. Therefore, bio-conjugation offers a route to achieving protein stability and catalytic efficiency in non-native media (Tung, C, Fung, & Li, 2016). It has been shown previously that surfactant coating can plasticise the structure of proteins in a manner analogous to water hydration (Correia Carreira, 2017), allowing it to function in non-aqueous solutions. This is significant, as typically this would result in a loss of protein flexibility and function, resulting in impairment of protein dynamics. Such an effect may manifest in an inability to access the different conformational states required by an enzyme for catalytic activity (Fogarty & Laage, 2014). The structure and folding of enzyme conjugates must therefore be investigate using appropriate biophysical methods, such as circular dichroism (CD) spectroscopy, in order to determine whether the protein conjugate resembles the native hydrated protein.

1.6 Research Aims

The ambition of this project was to apply bioconjugation methods to the natural Diels-Alderase AbyU, to generate polymer conjugated variants of this industrially relevant enzyme. The resulting protein-polymer conjugates were to be tested for tolerance to ‘harsh’ reaction conditions, akin to those commonly employed in process chemistry workflows. Finally, the impact of conjugation on AbyU catalytic function was to be assessed to establish the impact of conjugation of the kinetic properties of AbyU. Significantly, this research will lay the foundation for modifying AbyU and related beta-barrel Diels-Alderases for use in industrial biocatalytic processes.

Chapter 2. Materials and Methods

2.1 Protein Expression

10 mL LB containing 100 $\mu g.mL^{-1}$ carbenicillin was inoculated with an individual colony of *E. coli* BL21 (DE3) cells pre-transformed with pOPINF::AbyU (gift from Carl Marsh, University of Bristol). This inoculum was cultured with shaking at 200 rpm overnight at 37°C. This culture was transferred to 1 L LB containing 100 $\mu g.mL^{-1}$ carbenicillin, which was subsequently grown with shaking at 200 rpm at 37°C until an OD_{600nm} of 0.5 was obtained. The culture was cold shocked on ice for 15 minutes. Protein expression was *via* the addition of 1 mM IPTG (final concentration). The culture was then grown at 18°C with shaking at 200 rpm for 18 hours. Cells were recovered by centrifugation at 4600 g for 25 minutes. Cell pellets were archived at -80°C before being subjected to lysis.

2.2 Protein Preparation

Cell pellets were defrosted and re-suspended in 40 mL of Load buffer (50 mM Tris-HCl, 150 mM NaCl, 20 mM imidazole, pH 7.5). Suspensions were lysed by passage through a cell disruptor (Constant Systems Ltd). The recovered lysate was clarified by centrifuging for 30 minutes at 38,000 g and the supernatant decanted and loaded onto a nickel charged 5 mL HisTrap FF column (GE life sciences). Contaminating proteins were removed by washing with 8 column volumes of Load buffer. Protein bound to the column was eluted over 30 mL using a linear gradient of 0-50% Load to Elute buffer (150 mM NaCl, 20 mM Tris-HCl, 1 M imidazole, pH 7.5), collecting 1.5 mL fractions throughout the process. Fractions were analysed by absorbance at 280 nm of the column eluent followed by SDS-PAGE analysis of recovered fractions. Fractions containing AbyU at >70 % purity were mixed and concentrated to 2 mL by centrifugation. The resulting pooled protein was applied to a GE Healthcare 16/60 S75 column, pre-equilibrated in SEC buffer (150 mM NaCl, 20 mM Tris-HCl, pH 7.5). Elution was by passage of 120 mL of buffer through the column, with 1.5 mL fractions collected from 40–120 mL. Fractions were analysed by absorbance of the column

eluent at 280 nm, with fractions subsequently evaluated by SDS-PAGE. Fractions estimated to be of >95 % purity were pooled and concentrated to 10 mg.mL^{-1}. 100 μL aliquots of this material were flash frozen and archived at -80°C.

2.3 Protein Modification

Solutions of recombinant AbyU (2 mg. mL^{-1}) were passed through a 0.22 μm syringe filter and then incubated with a 200 mg. mL^{-1} solution of N,N-dimethyl-1,3-propanediamine (DMPA) at pH 6, maintained by addition of 6 M HCl in a fume hood. The solutions were continuously stirred for 4 h, following which EDC solid was added and the sample stirred for an additional 4 h. Aspartic/glutamic acid residues in AbyU were cationised using an EDC zero-length crosslinker and DMPA as the cationising amine. Generally, the amine was diluted to a concentration 150 times molar concentration of the protein and then brought to pH 6 using HCl (6 M), after which it was added to a 2 mL solution of AbyU dissolved in 20 mM phosphate buffer. A 34-fold excess of EDC. HCl was added, followed by a second addition of this reagent after a 4 h interval, to maintain the reaction. The protein was subsequently dialysed against 4 L of 20 mM phosphate buffer (pH 7.5) at 4°C overnight, to produce stable solutions of the DMPA-cationised protein, with frequent water changes over a 24-hour period. Aggregates were removed using a 0.22 μm filter. 2.5 mL of the dialysed cationised protein was loaded onto a Centrisart 10K CTA column. Modified AbyU was eluted from the column *via* passage of 25 mL of buffer through the column under gravity. Protein recovery was quantified by UV-vis spectrometry. The degree of cationisation was determined using MALDI Time of Flight (ToF) mass spectrometry. [C-AbyU] was stored at 4°C following preparation but prior to experimentation.

The glycolic acid ethoxylate 4-nonylphenyl ether surfactant, IGEPAL CO-890 (Figure 2.1) was synthesised by the oxidation of the hydroxyl groups of a glycolic acid ethoxylate 4-nonylphenyl ether to yield a carboxylic acid terminus. Complexation of the anionic polymer surfactant (Figure 2.2) was carried out at a ratio of 1 surfactant chain per newly cationised site, to ensure high conjugation efficiency and prevent surfactant self-association. The protein solution was stirred for 2 hours with a 10 mg.mL^{-1} of oxidised IGEPAL CO-890 in 20 mM of the reauisite buffer at 4 °C.

The resulting protein-surfactant solution was centrifuged to remove any aggregates. Size exclusion chromatography was carried out to select for protein populations that were homogenously conjugated and to remove any excess surfactant. The resulting solution was stored at 4 °C. The concentrations of [C-AbyU]and [C-AbyU][S] were estimated using a BCA assay and/or Bradford assay.

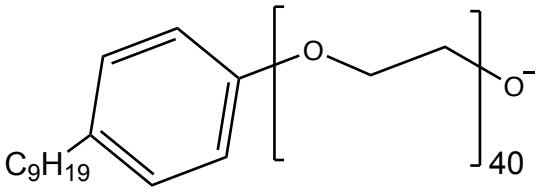

Figure 2.1 Chemical structure of the surfactant, IGEPAL CO-890 (MW ~1,982 Da).

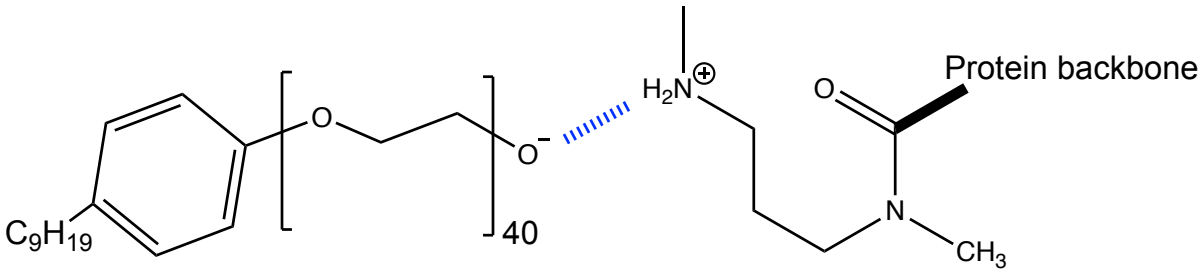

Surfactant polymer IGEPAL-890

Figure 2.2 Complexation of oxidised polymer surfactant with cationised protein sidechain. The electrostatic interaction between the anionic polymer and positively charged coupled diamine is shown as a dashed blue line.

2.4 BCA Assay

Serial dilutions of a Bovine Serum Albumin (BSA) standard stock solution (2mg.mL^{-1}) were performed as recommended by the manufacturer (ThermoScientific). The total volume of working reagent (WR) required was calculated according as follows;

(# standards + # unknowns) × (# replicates) × (volume of WR per sample) = total volume WR required

2 mL of WR is needed per sample. In this case, there were 10 standards, 2 unknowns and 3 replicates, requiring 72 mL of WR. The BCA reagents A and B were mixed in a 50:1 ratio and vortexed to mix well. 25 μL of each sample (standard and unknown) was pipetted into a 96-well plate well. 200 μL BCA WR was then pipetted into each well of the plate. Plates were then sealed and incubated for 30 minutes at 37 °C, then left to cool for 5 minutes. The absorbance of each sample well was determined at 562 nm using a plate reader (Synergy™ BioTek HTX Multi-Mode Reader). A standard graph was generated using the formula y = mx + c.

2.5 Bradford Assay

Bradford assays were performed according to a standard assay procedure using 96-well microarray plate. A 2 $mg.mL^{-1}$ BSA standard was used and diluted as detailed by the manufacturer (Thermofisher). Samples were assayed in triplicate. Blank samples were made using Milli Q grade water and dye reagent. Sample solutions, both standards and unknowns were pipetted into individual wells. A multichannel pipette was used to dispense the 1x dye reagent, with sample mixing achieved by repeated pipetting. Samples were incubated for 5 minutes at 20°C and followed by measurement of absorbance at 595 nm.

2.6 Substrate Synthesis

The AbyU substrate was synthesised and purified by Li-Chen Han of the Willis group, School of Chemistry, University of Bristol according to literature syntheses (Byrne et al., 2016). The resulting solutions of substrate were purified to a concentration of 60 mM. Substrate solutions were stored at -80°C to prevent spontaneous cyclisation.

2.7 SDS-PAGE

10 µL protein solutions were heated to 100°C for 10 minutes in 10x sample buffer (Thermofisher). 10 µL samples were loaded onto 15% NuSEP Tris–glycine gels. Gels were electrophoresed using a Mini Protein II gel apparatus (Bio-Rad) employing Tris–glycine running buffer at 150 V over 50 minutes.

2.8 NATIVE-PAGE

Samples were prepared by mixing equal quantities of protein solution and sample buffer (87 mM Tris-HCl, 0.2% bromophenol blue and 0.004% glycerol, 1 mM DTT). Samples were then loaded into the wells of a 10% native polyacrylamide gel. Gels comprised 375 mM Tris-glycine, pH 8.8 (resolving gel), and 625 mM Tris-glycine, pH 6.8 (stacking gel). Gels were electrophoresed in running buffer (0.19 M glycine, 25 mM Tris-HCl, pH 8.8) at 15 V for 150 minutes.

2.9 Liquid Chromatography-Mass Spectrometry

Chromatographic separations were performed using a 5 µm C_{18} 100 Å, 4.6 x 250 LUNA column (Phenomenex), using a linear gradient of 10-90% acetonitrile/0.5% formic acid over 15 minutes. Mass spectrometry was performed using a Waters ZQ Micromass spectrometer in positive ion mode. Molecular masses were determined b mass spectrometry, with the assistance of Li-Chen Han (Chemistry, Bristol).

2.10 Zeta Potential Measurements

Cationisation efficiencies were assessed qualitatively using dynamic light scattering (DLS) coupled with zeta potential measurements, with protein samples at 1 $mg.mL^{-1}$ final concentration using a Malvern Nano-Z instrument. An average of 100 runs per sample were collected and averaged. The zeta potential of the 20 mM phosphate buffer at pH 7 [-10 mV] was determined and subtracted from final zeta potential measurements. Cationisation was verified by a change in zeta potential. It is expected

that the zeta potential will become more positive once the protein has been cationised due to an increase in surface electrostatics. Following conjugation, the zeta potential should return to ~0 mV, since the surfactant will have attached to the positively charged amino acids on the protein surface.

2.11 Matrix-Assisted Laser Desorption / Ionisation Mass Spectrometry (MALDI-MS)

Molecular masses of native and cationised proteins were measured using MALDI-MS using an Applied Biosystems 4700 Proteomics Analyser). Mass spectroscopy enabled calculation of the average number of DMPA (MW 100 Da) molecules bound per cationised protein molecule. Non-cationised AbyU was used as the background control. Each 100 Da increase in mass has taken to corelate to the addition of a single molecule of DMPA. For example, a mass increase of ~500 Da detected after cationisation was taken as equating to the addition of 5 DMPA molecules. Porcine trypsin (Sequencing-grade, Promega) was dissolved in 50 mM acetic acid, followed by 5-fold dilution, achieved by adding 25 mM ammonium bicarbonate. The final concentration of trypsin used was 0.02 $\mu g.\mu L^{-1}$. 10 μL of this protease solution was mixed with each protein sample, followed by incubation at 37 °C overnight. 1 μL aliquots of each digest preparation was applied to the ground steel MALDI target plate, with this application followed immediately with an equal volume of 4-hydroxy-α-cyano-cinnamic acid (freshly-prepared, 5 $mg.mL^{-1}$, Sigma Aldrich) suspended in 50% aqueous (v/v) acetonitrile, supplemented with 0.1%, trifluoroacetic acid (v/v). Analyses were performed using a Bruker ultraflex III MALDI mass spectrometer in positive-ion mode, fitted with a Nd:YAG smart beam laser. All spectra were acquired over a mass range of m/z 800-4000 using FLEX Control software (Bruker, USA) and peaks were identified using FLEX Analysis software (Bruker, USA).

2.12 Tryptic Digest

For tryptic digest analysis of proteins, 20 µg samples of the cationised AbyU polypeptide were added to 80 µL of 20 mM Tris-HCl, pH 8. 5 µL of 200 mM TCEP was

added followed by incubation at 55 °C for 1 hr. 10 µL of a 400 mM iodoacetamide stock solution was added to the buffered protein solution, which was then incubated for 1 hr at 25 ^{o}C. Following incubation 10 µL of 400 mM DTT was added and samples were incubated at RT for a further 1 hr. 1 µg Trypsin was added to solution and a final incubation at 37 °C overnight performed. The digested sample was resuspended in 5% formic acid followed by desalting on a SepPak cartridge (Waters). The eluate from the cartridge was evaporated and resuspended in 1% formic acid in preparation for nano-LC MS/MS analysis. Samples were fractionated using an Ultimate 3000 nano-LC system fitted with an LTQ-Orbitrap Velos mass spectrometer (Thermo Scientific). Peptides in 1% (vol/vol) formic acid were next loaded onto a 250 mm × 75 µm Acclaim PepMap C18 nano-trap column (Thermo Scientific) which was then washed with 0.5% (vol/vol) acetonitrile 0.1% (vol/vol) formic acid. Peptides purification was performed using a previously reported standard regime (Fu et al., 2017). Solvent A comprised 0.1% formic acid; Solvent B comprised 80% acetonitrile with 0.1% formic acid. Resolved peptides were ionized using nano-electrospray ionization at 2.1 kV employing a 30 µm diameter stainless-steel emitter (Thermo Scientific) at 250 °C. Tandem mass spectroscopy analysis was undertaken using an LTQ-Orbitrap Velos mass spectrometer in data-dependent acquisition mode, controlled using Xcalibur 2.1 software (Thermo Scientific). Survey scans were performed at 60,000 resolution (m/z 400) in the mass range ofm/z 300 – 2000. In each duty cycle the top ten multiply charged ions in the LTQ linear ion trap were selected for MS/MS. Charge state filtering and dynamic exclusion were applied during analysis. The following fragmentation conditions in the LTQ were used: normalized collision energy, 40%; activation q, 0.25; activation time 10ms; and minimum ion selection intensity, 500 counts. All output data were processed and quantified in Proteome Discoverer software v1.4 (Thermo Scientific). Mass results were searched against the UniProt *V. maris* strain AB-18-032 database (6006 entries) applying the SEQUEST algorithm. The mass tolerance value was set at 10 nppm; the MS/MS tolerance value was set to be 0.8 Da. Search criteria included carbamidomethylation of cysteine (+57.0214) as a fixed modification and oxidation of methionine (+15.9949 Da) and the DMPA modification of aspartic and glutamic acid (+84.105 Da) as variable modifications. Mass searches included complete tryptic digestion, incorporating a maximum tolerance of 2 missed cleavages permissible. Searches were performed with the reverse database search option

active, with all peptide data filtered to ensure a maximum false discovery rate (FDR) of no greater than 1%.

2.13 Small Angle X-Ray Scattering (SAXS) Techniques

SAXS measurements were undertaken on beamline B21 at Diamond Light Source (Harwell, UK) fitted with a BIOSAXS robot for automated sample loading and recovery. Protein samples were transferred to the 96-position sample holder of the EMBL BioSAXS robot. Loaded samples were auto-injected into a 1.8 mm interal diameter quartz capillary positioned perpendicularly to the X-ray beam. The quartz capillary was housed in a vacuum chamber to minimise scattering artefacts. Scattering data were collected using a fixed camera length (4.014 m) and energy (12.4 keV). Scattering images were recorded on a PILATUS 2M detector. Sample concentrations for scattering experiments were as follows: 1, 0.5, and 0.25 and 0.125 $mg.mL^{-1}$ for buffered WT AbyU; 1 $mg.mL^{-1}$ for buffered conjugated AbyU. Samples were exposed for 15s, collecting 18 frames at 20°C. Following data collection individual frames were sector-integrated. As a consequence of the absence concentration-dependent effects, all data were collected from AbyU samples at 1 $mg.mL^{-1}$. Scattering from buffer only samples was subtracted from AbyU samples on the beam-line using SCATTER. Maximum intra-particle dimensions (D_{max}) and particle distance distribution functions ($p(r)$) were calculated using the programme GNOM (Svergun, 1992). Radius of gyration (R_g) calculations were carried out using PRIMUS (Petoukhov, 2012), applying the Guinier approximation and were used to generate a Kratky plots. *Ab initio* protein models (13 total) were produced using DAMMIF/DAMMIN and averaged using DAMAVER in the ATSAS suite (Franke & Svergun, DAMMIF, a program for rapid ab-initio shape determination in small-angle scattering. , 2009). The final model was superposed to the AbyU structure (PDB ID:5DYV) using SUPCOMB (Franke, et al., 2017).

2.14 UV/Visible Spectroscopy

Samples were diluted in 20 mM of the corresponding buffer, and absorbance measurements were taken over the wavelength range λ = 200-600 nm using a

Lambda 25 spectrophotometer (Perkin Elmer, USA). The Beer-Lambert law was used to determine protein concentration, according to the following equation:

$$A = \varepsilon cL$$

accounting for path length (L), the absorbance intensity (A_{280}) at λ = 280 nm and the extinction coefficients (ε_{280}) of 25440 $M^{-1}cm^{-1}$ for native AbyU (Protein Calculator, Scripps Research Institute).

2.15 Synchrotron Radiation Circular Dichroism (CD) Spectroscopy

Near and far-UV circular dichroism spectroscopy was performed using Beamline B23 running Global Works software (Olis, USA) at Diamond Light Source. Samples were diluted in the corresponding buffer, then scanned between λ = 180-260 nm in 1 nm increments with 4 second integration times. The temperature was kept constant at 25°C, except during thermal unfolding experiments, in which case the temperature was incrementally increased to 95 °C using a Peltier Temperature controller (Quantum, USA) in 5°C increments. Prior to each scan, the temperature was allowed to equilibrate for five minutes. All circular dichroism data is reported in units of mean residue molar ellipticity (θ_{MR}). This was calculated by normalising the circular dichroism (ΔA) signal with respect to sample concentration (C), pathlength (L) and number of amino acids (N), according to the following equation:

$$\theta_{MR} = \frac{\text{millidegrees (m°) x M (g.mol}^{-1}\text{)}}{10 \text{ x L x C (g.L}^{-1}\text{)}/_{N}} \quad [2]$$

Where M is the average molecular weight of the protein

C = molar concentration ($mg.ml^{-1}$)

2.16 Chemical Denaturation Studies

Chemical denaturation studies were performed my monitoring the change in environment of the 3 tryptophan residues of AbyU. A change in fluorescence denotes exposure of the tryptophan residues to solvent and indicates protein unfolding. A stock solution of GuHCl (6 M) was prepared in 20 mM Sodium phosphate buffer, pH 7.5, and serially diluted using buffer to prepare a series of solutions containing different concentrations of GuHCl. The mean residue ellipticities of the different solutions were measured at 20°C using a fluorometer at an excitation wavelength of 290 nm. Emission acquisition scans were from 310-400 nm. For each concentration of GuHCl, 3 scans were taken and averaged. The free energy of unfolding at different denaturant concentrations (ΔG_u) was established using the equation:

$$\Delta G_u = -RT\ln(f/l - f) \quad [3]$$

Where G_u = the free energy of unfolding

R = gas constant

T = temperature constant in Kelvin

These values were then plotted vs. concentration of denaturant. Estimates of the free energy of unfolding without denaturant present (ΔG_u^{H2O}) were obtained by a linear extrapolation.

Unfolding data were fitted according to the Fersht equation:

$$Y = \frac{(sN+sD)\exp\left(\frac{mX-\Delta G}{0.59}\right)}{1+\exp\left(\frac{mX-\Delta G}{0.59}\right)} \quad [4]$$

Where sN = signal at maximum native

sD = signal at maximum denatured

X = denaturant concentration

M = m-value

m = cooperative unfolding constant.

Measurements (*n*=3) of the catalytic activity of native AbyU were carried out in increasing concentrations of GuHCl to assess enzyme tolerance to denaturant. The reaction was allowed to equilibrate for 1 minute, and initial velocity was measured.

2.17 Enzyme Activity Assays

Reaction rates for the conversion of substrate to product in the presence or absence of native and modified AbyU were determined spectrophotometrically by monitoring the rate of substrate disappearance at 325 nm, employing an extinction coefficient of 18400 $M^{-1}cm^{-1}$. The rate of the AbyU catalysed and non-catalysed reactions were calculated by monitoring the change in absorbance for 1 minute at substrate concentrations of 0, 50, 75, 100, 150 and 200 µM. A second set of reactions were carried out using a quartz cuvette of 1 mm pathlength, a 1 µM concentration of enzyme in a total volume of 400 µL. This was to investigate enzyme kinetics at higher substrate concentrations (100, 200, 300, 400, 500 µM) in order to saturate the enzyme active site and calculate enzyme parameters (k_{cat}, K_m). All assays were performed in reaction buffer comprising 20 mM phosphate, 150 mM NaCl, pH 7.5, at 20 °C. Preliminary AbyU enzyme activity assays were undertaken using an assay volume of 125 µL in 10% acetonitrile, using a 1 cm pathlength quartz cuvette. In subsequent analyses of the modified AbyU catalysed reaction, a high-throughput screening method was employed using a UV-visible spectrometer plate reader. Low volume absorbance assays were carried out in a 96-well plate, over a period of 5 minutes. Readings were taken at 25 second intervals for substrate concentrations in the range 0, 25, 50, 75, 100, 150, 200 and 250 µM. 7 µL of 1 µM enzyme was added to each well, which

contained 10% acetonitrile in a total volume of 100 μL buffer. The absorbance of each well solution was monitored continuously using a microplate reader by monitoring the loss of absorbance signal at 325 nm. The intensity values were converted to concentration values using the standard curve, and initial velocities for each assay were determined by normalizing the data to the 10% acetonitrile buffer control. A 60 mM stock solution of AbyU substrate was diluted 1 in 10 and dissolved in 50% acetonitrile to give a 6 mM working stock of substrate. This was accounted for during assay preparation to ensure 10% acetonitrile concentration for each reaction condition. All assays were initiated by the addition of cold substrate (4 °C) to pre-prepared reaction mixes. The reaction velocities of native, cationised and conjugated enzyme at a final concentration of 1 μM were analysed. Controls were performed using identical assay mixes and reaction conditions, but either excluding enzyme, or using heat denatured native enzyme and heat denatured modified enzymes. Heat denatured samples were heated to 95 °C and checked for loss of secondary structure using CD spectrometry.

For non-enzymatically catalysed reactions the resulting data were fitted to an equation of the form:

$$[A] = [A_0]e^{-kt} \quad [5]$$

Where [*A*] = the concentration of substrate at time *t*

[A_0] = the concentration of substrate at time 0

k = the reaction rate.

For enzymatically catalysed reactions, the data were fitted to the following equation:

$$v_0 = \frac{k_{cat}[E][A]}{k_{m+[A]}} \quad [6]$$

Where v_0 = initial velocity

[E] = enzyme concentration

[A] = substrate concentration at time 0

k_{cat} = the enzyme catalysed reaction rate

K_m = the Michaelis constant.

All reactions were repeated in triplicate. Data fitting was performed using GraphPad Prism.

2.18 Activity Assay Data Analysis

Catalytic activities of native and modified AbyU at 25 °C were determined from mean average (n=3) initial reaction rates by linear regression analysis. Turnover rates were derived from absorbance changes at 325 nm at defined time points post substrate addition (averages of n=3). This was calculated by dividing substrate concentration (ε_{325}=36930 M^{-1} cm^{-1}) by the concentration of enzyme active sites. Absolute values for enzyme and substrate concentrations within assay mixes were calculated from constituent mass fractions. Activities were derived from experimentally determined initial by plotting A_{325} vs. time at varying substrate concentrations. Normalised data were fitted to an exponential function to mitigate variations in absorbance readings. Resulting plots of rate vs. concentration were expressed as the initial rate/enzyme concentration (v_i/[E]) vs. substrate concentration.

Chapter 3. Results and Discussion

3.1 Expression and Purification of AbyU

AbyU was recombinantly over-expressed in *E. coli* strain BL21(DE3) and the resulting protein then purified using nickel affinity chromatography (Figure 3.1) followed by size exclusion chromatography (SEC) (Figure 3.3). SDS-PAGE analysis of fractions eluted from each chromatographic step demonstrated the effectiveness of the purification strategy employed (Figures 3.2 and 3.4), which yielded an AbyU preparation of >95% purity.

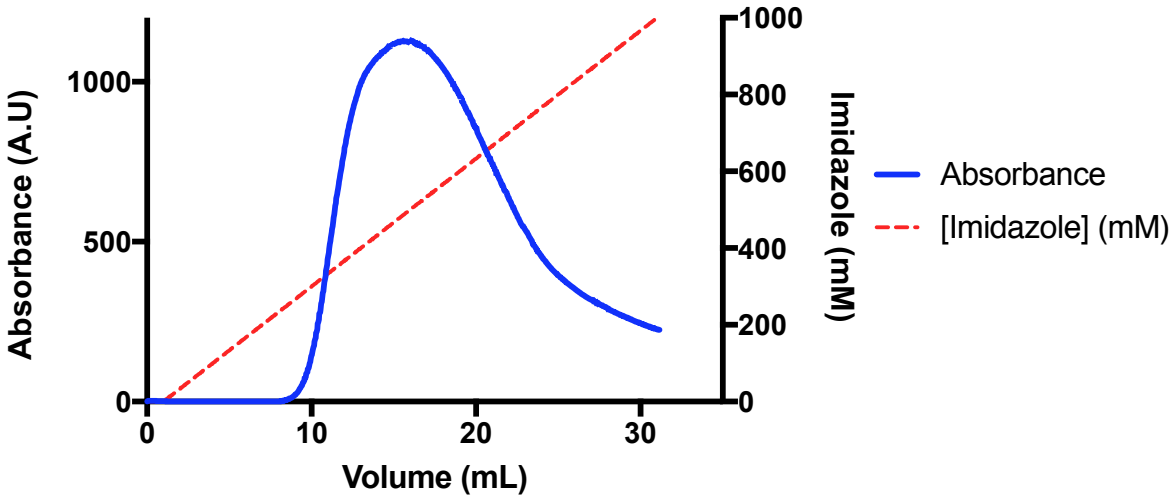

Figure 3.1 Ni-NTA affinity purification of AbyU. A chromatogram showing the purification of AbyU monitoring the column eluent at 280 nm.

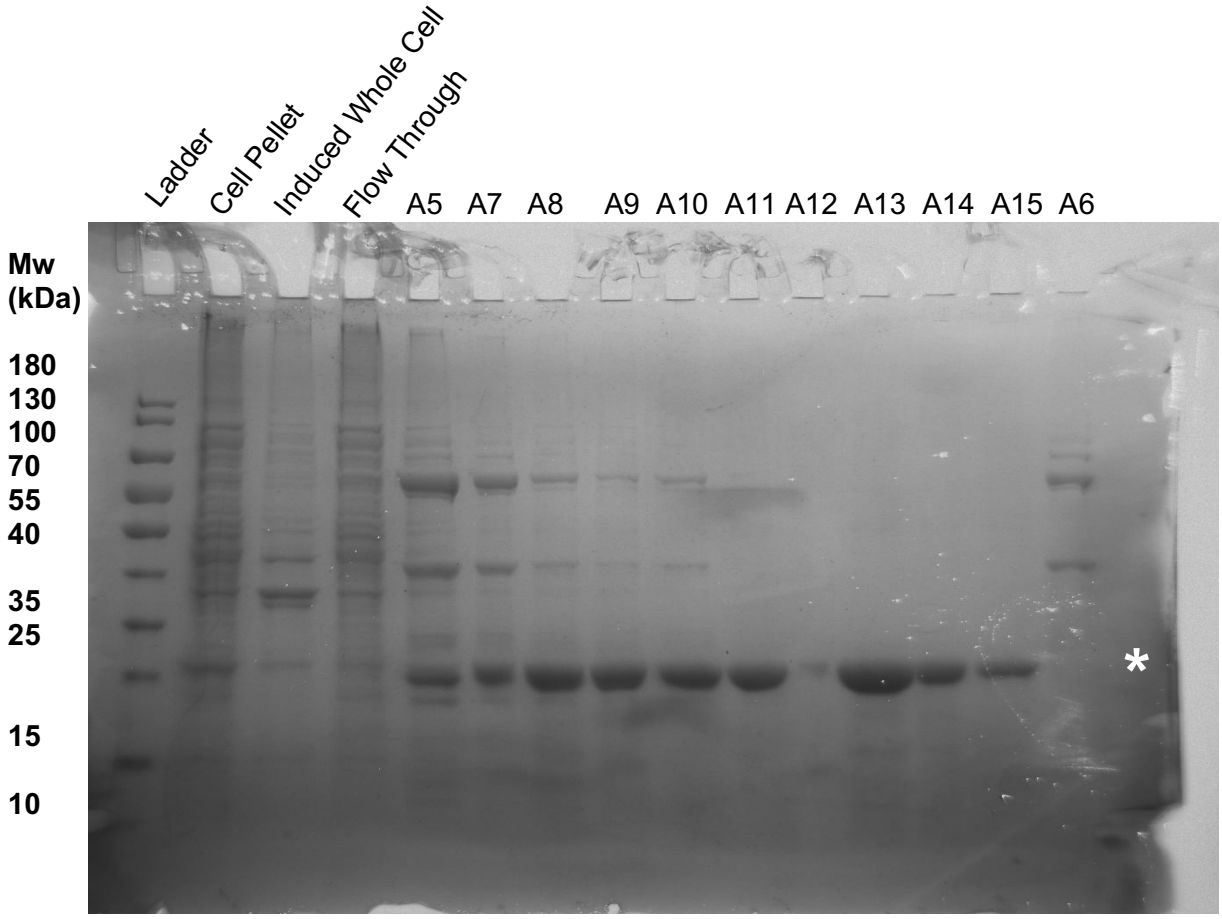

Figure 3.2 SDS-PAGE analysis of Ni-affinity purification of AbyU. Cell lysate generated from *E. coli* expressing recombinant His-tagged AbyU was fractionated using Ni-NTA affinity chromatography and the proteins in each fraction analysed by SDS-PAGE. The theoretical molecular weight of an AbyU monomer with an attached hexa-his tag is ~17.7kDa. The expected position of migration is indicated by the white asterisk.

The eluted fractions correspond to the method used to purify protein. Fraction A5 corresponds to roughly 300 mM imidazole, and the following fractions were collected at 1 mL intervals.

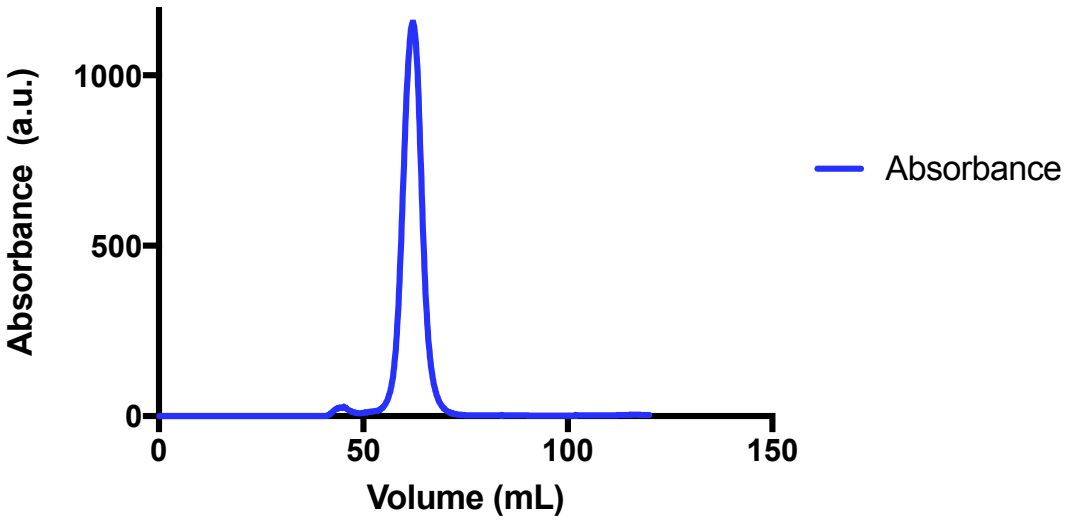

Figure 3.3 Size exclusion chromatogram of purified recombinant AbyU. The chromatogram shows the elution profile of AbyU from a Superdex 75 10/300 column (GE Healthcare). The buffer used for purification was 20 mM Tris-HCl, 150 mM NaCl, pH 7.5. 2.5 $mg.mL^{-1}$ of protein was loaded onto the column. Eluted peaks were observed by monitoring the absorbance of the column eluent at 280 nm. A single protein species is observed eluted from the column shown by the single peak.

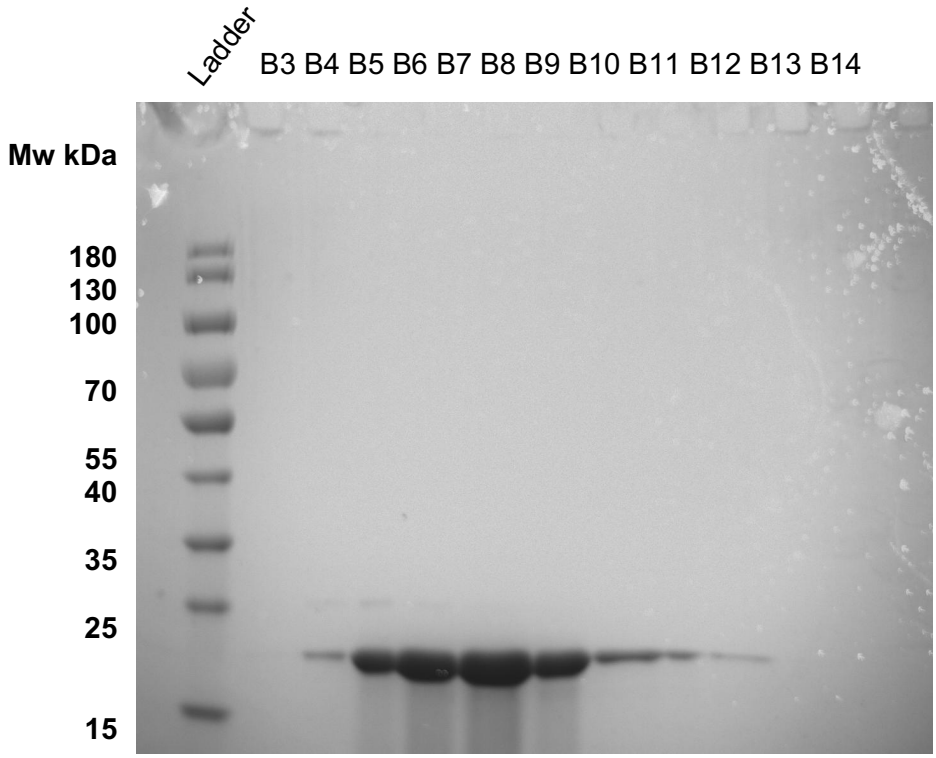

Figure 3.4 SDS-PAGE analysis of SEC column fractions. Fractions were eluted from a superdex S75 10/300 column. The apparent molecular weight of AbyU is ~17.7 kDa with the associated tag.

Fraction B3 corresponds to roughly 55 mL column eluted, and the following fractions were collected at 1 mL intervals. Fraction B7 corresponds to the apex of the elution peak shown in Figure 3.3.

3.2 Protein Quantitation

Fractions containing AbyU, recovered following SEC purification, were pooled and the concentration of protein in the pooled fractions was determined. This was done by measuring the absorbance of the solution at 280 nm, or by BCA or Bradford assay, through comparison with a protein standard (Figures 3.5 and 3.6 respectively).

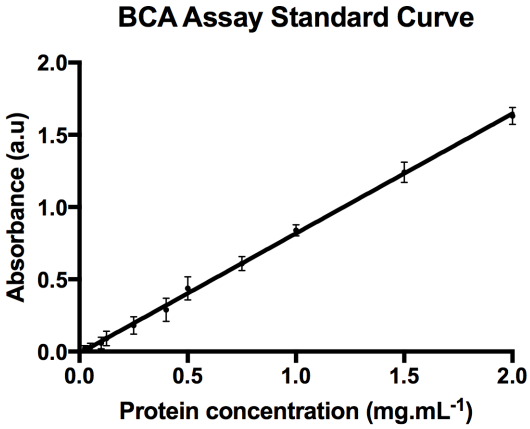

Figure 3.5 BCA assay standard curve used to estimate protein concentration. Estimated based on the absorbance of the protein standard BSA measured at 562 nm. The plot was generated using the formula y = mx + c*, n*=3 (where *n* is the number of repeats).

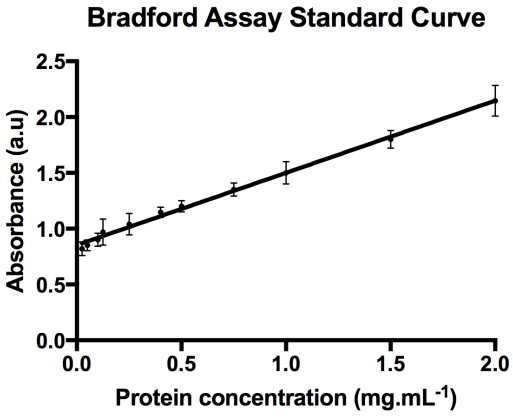

Figure 3.6 Bradford assay standard curve for measurement of protein concentration. The plot was generated using the formula y = mx + c, *n*=3.

The total yield from the protein preparation was ~15 $mg.mL^{-1}$. The results of the protein preparation using absorbance at 280 nm to estimate the native AbyU protein yield were similar to that of the BCA and Bradford assays. Following cationisation and conjugation, the protein might precipitate due to the harsh reaction conditions of the modification process. Therefore, the yield of native AbyU during preparation is likely to be higher than the cationised and conjugated proteins.

The absorbance at 280 nm could not be used following cationisation and conjugation due to the surfactant polymer interfering with the signal at 280 nm. This is because the polymer also absorbs at 280 nm, so the total reading will be much higher than the amount of protein present in the samples. The BCA and Bradford assays were therefore the best techniques available to estimate protein concentration after cationisation and conjugation.

3.3 Validating Cationisation

Following purification and quantitation of recombinant AbyU, the cationisation efficiency of DMPA-coupling to the enzyme was determined using two techniques; 1) zeta potentiometry and 2) matrix-assisted laser desorption ionization time-of-flight (MALDI-TOF) mass spectrometry. The two-step bioconjugation was achieved by the covalent coupling of *N,N'*-dimethyl-1,3-propanediamine (DMPA) to the side chains of acidic amino acids within AbyU, to form the cationised protein. These residues were in turn electrostatically conjugated to the anionic polymer–surfactant glycolic acid ethoxylate 4-nonylphenyl ether ($H_{19}C_9$-Ph-O-$(CH_2CH_2O)_{40}$-CH_2-COO-) to produce hybrid protein-surfactant complexes. Zeta potential measurements confirmed that cationisation had yielded an AbyU derivative with a predominately positively charged surface, which had been neutralised following surfactant conjugation (Figure 3.7). The efficiency of cationisation of was determined using mass spectrometry. Analysis of these data were consistent with the addition of ~20 molecules of DMPA (Figure 3.8).

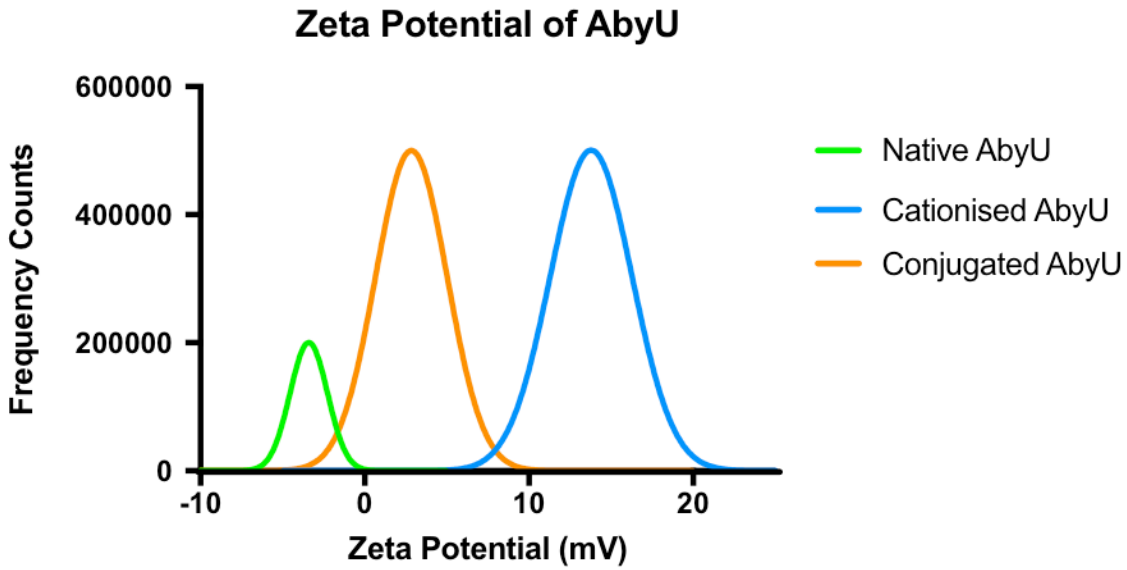

Figure 3.7 Zeta potential spectrometry of modified AbyU enzymes. *n*=5, where n=number of measurements. The plot is a mean average trace. The zeta potential changed from -3.34 mV ± 0.3 for native AbyU to + 13.67 mV ± 0.7 for [C-AbyU], consistent with the switching of the polypeptide's surface potential from negative to positive. The zeta potential for [C-AbyU][S] was + 2.85 mV ± 0.8, which shows that the positive charge on the surface of [C-AbyU] decreased following conjugation.

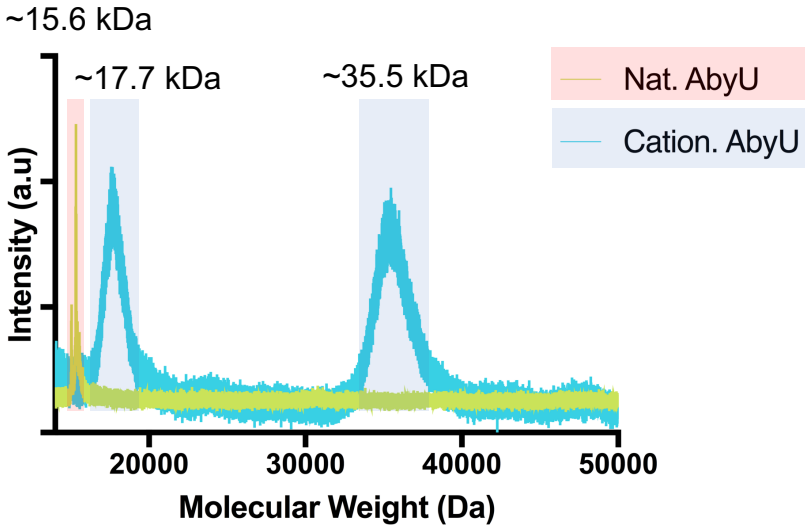

Figure 3.8 Mass spectrometry of AbyU and [C-AbyU]. Mass-to-charge (m/z) spectrum of AbyU and [C-AbyU] generated by MALDI-TOF. The natural AbyU, tag-cleaved molecular weight ~15.6 kDa, is shown to be a monomer under MALDI-TOF conditions. However, in solution AbyU forms a dimer. A mass increase from 15.6 kDa to 17.7 kDa is observed after cationisation. Two species of [C-AbyU] are seen, appearing at ~17.7 kDa and ~35.5 kDa. It may be that the conditions of MALDI-TOF promotes dimerisation of the cationised protein, which could explain the two peaks seen.

Mass spectrometry experiments identified a subunit molecular weight of 15.6 kDa for native (un-tagged) AbyU and 17.7 kDa for [C-AbyU]. This mass increase equates to ~20 DMPA (MW ~100 Da) molecules/protein monomer, and hence cationisation of 20 acidic residues within the protein.

3.4 Identification of Cationised Sites

Tryptic digests were performed on [N-AbyU] and [C-AbyU] to determine which amino acid residues had been modified by DMPA. The enzyme trypsin is used to digest protein into smaller peptides, which can then be analysed by matrix-assisted laser desorption ionization mass spectrometry (MALDI-MS), enabling quantitation their mass and establishment of their identity. Trypsin preferentially cleaves lysine and arginine residues in the N-to C-terminal direction. There are 13 cleavage sites in the AbyU sequence, releasing 14 peptides of varying lengths. This type of analysis is useful as it gives explicit information on which side chains are being modified, aided by the differences between the peptide mass fingerprints of [N-AbyU] and [C-AbyU]. The resulting changes in masses of the individual peptide fragments were able to elucidate which side chains DMPA attached to (Table 3.4).

An increase in peptide mass of ~84.05 Da is seen following cationisation (Table 3.4) at a specific site, which can be attributed to DMPA addition (+84.105 Da) to acidic residues. Retention times of modified fragments were shorter than native peptide fragments, which can be explained by the increase in positive charge caused by DMPA, as retention time has been shown to decrease dramatically with an increase in the number of positive charges within the peptide fragments (Mant & Hodges, 2006). This is evidenced by peptides that were not modified in [C-AbyU], which retain the same masses and retention times as in [N-AbyU]. The LCMS analysis revealed that the modifications occurred mainly in the beta motif and turns (Figure 3.9). It is expected that the chains being modified would be those that are solvent accessible, for example residues on the outside of the barrel.

Peptide Sequence	Position	#Missed Cleavages	#Modifications	Modifications	MH+ (Da) [N-AbyU]	MH+ (Da) [C-AbyU]	Retention Time (min) [N-AbyU]	Retention Time (min) [C-AbyU]
LETRPQALLIKVPTEIVVK	5-23	1	0		2147.320	2147.318	92.17	92.35
VVddVdVAAPAVGQVGK	24-40	0	3	D3 (DMPA)	1638.874	1722.977	75.83	57.58
				D4 (DMPA)	1638.874	1722.977	75.83	57.34
				D6 (DMPA)	1638.874	1722.978	75.83	58.79
FDDeLYdeAGAQIGTSSGNFR	41-61	0	3	E4 (DMPA)	2292.005	2376.116	105.49	86.79
				D7 (DMPA)	2292.005	2376.110	105.47	86.77
				E8 (DMPA)	2292.005	2376.110	105.47	86.77
TSKWVFYPATGVSGR	100-114	1	0		1655.856	1655.856	79.08	79.46
SAEARILLGe	132-141	1	1	E10 (DMPA)	1058.585	1142.692	65.96	46.56

Table 3.1 Modifications to AbyU peptide sequences. Following cationisation, DMPA addition (+84.105 Da) to D and E residues increased peptide mass.

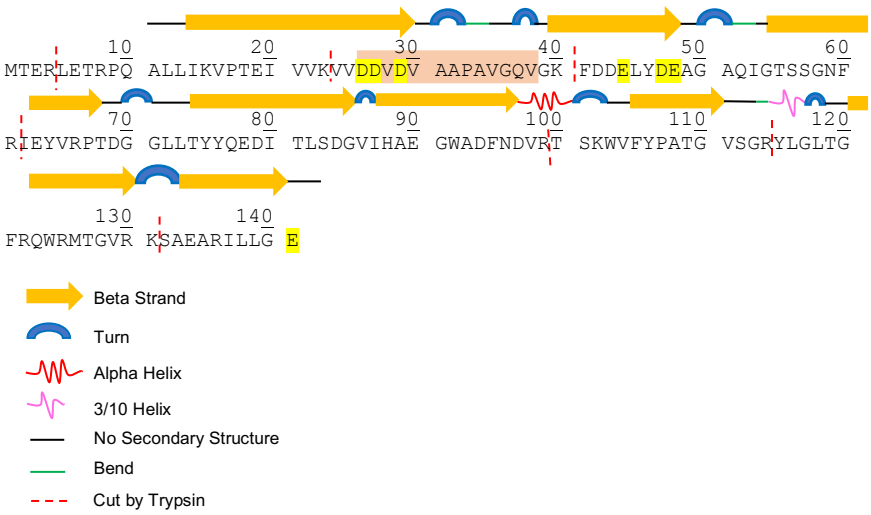

Figure 3.9 Protein sequence of AbyU showing secondary structure. DMPA modification sites are highlighted in yellow and capping loop residues are shaded in pink.

The peptide sequence, IEYVRPTDGGLLTYYQEDITLSDGVIHAEGWADFNDVR, was unable to be analysed by MALDI-TOF, as the ionised fragment was too large to be accelerated towards the mass spectrometer detector. This peptide equates to a region on the outside of the β-barrel where DMPA modification is expected to occur, therefore the proportion of DMPA-modified sites reported by the digest may not accurately reflect the true amount of DMPA coupling to aspartate and glutamate residues of AbyU. Since trypsin is unable to cleave this peptide into smaller fragments, a future experiment could use other proteases, such as pepsin (pH>2, 14 cleavage sites) or proteinase K (22 cleavage sites), to digest the sequence. However, this analysis reveals that DMPA modification is concentrated in flexible loop areas and on the outside of the barrel (Figure 3.10), being particularly evident on the capping loop. This suggests that these residues are susceptible to modification.

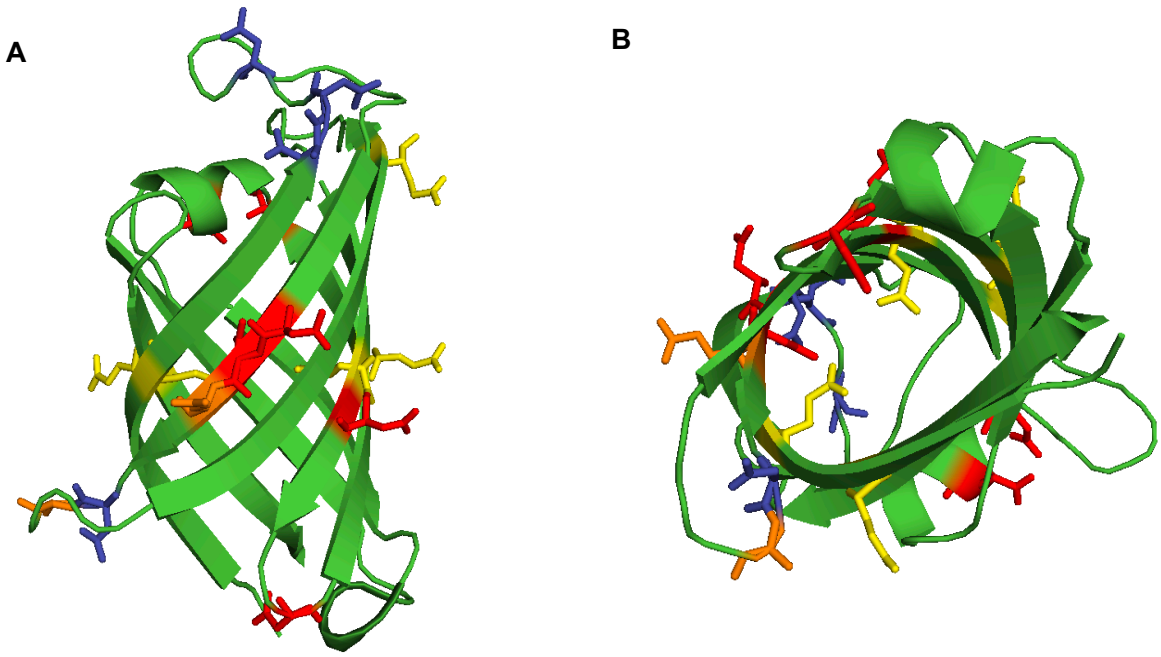

Figure 3.10 Location of the DMPA modification sites on AbyU. (A) Side-on view of modification sites in AbyU. **(B)** Top-down view of AbyU. DMPA-modified aspartates are shown in blue, modified glutamates are shown in orange. Yellow residues and red residues indicate unmodified glutamate and aspartate residues, respectively.

There are 3 amino acids (E19, D43, E78) inside the AbyU β-barrel core which could potentially react with DMPA (Figure 3.10). The digest revealed that these residues were not modified, which suggests that there is no DMPA addition within the enzyme active site. This is expected, as these residues are highly protected from solvent exposure through the action of the capping loop, making it unlikely that DMPA coupling would occur in this region. The data demonstrates that the 3 acidic residues in the enzyme active site were not modified and identifies those on the outside of the enzyme scaffold that were.

3.5 Validating Conjugation

SAXS and NATIVE-PAGE analysis were used to investigate conjugation success. SAXS is useful as it can provide nanoscale structural information about biomolecules (>30 kDa), describing parameters which include overall shape, particle size, samples homogeneity and surface to volume ratio (Hura, Menon, Hammel, Rambo, & Poole, 2009). X-rays are shone through a solution of protein, which scatters the incoming X-rays to give a scattering pattern, which is subsequently recorded on a detector (Figure 3.11). An electron density map is created based on the contrast between the protein and solvent, according to the equation $\Delta\rho(r) = \rho(r)$ protein - ρsolvent, where ρ describes the distance distribution function between particles either in the protein or in the solvent. The p(r) function averages the distance vectors within the particles from the statically measured samples and positions it into real space, to reveal protein dimensions.

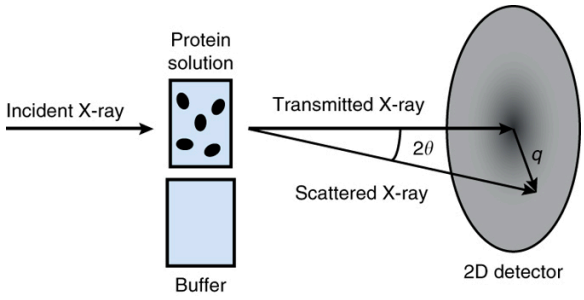

Figure 3.11 Principle of Small-angle X-ray scattering. Taken from *Polymer Journal* (Nozue, Shinohara, & Amemiya, 2007) in which the scatter signal of the buffer solution is background subtracted from the scatter signal of the protein solution.

SAXS can provide evidence for a protein's oligomeric state in solution, provide a low-resolution structural model describing shape (e.g. globular, ellipsoidal) and identify whether polypeptides are able to interact to form complexes. Significantly, SAXS data can propose a 3D representation of the protein by constructing an electron density envelope and fitting a high-resolution image of the protein structure within the calculated density (Figure 3.12).

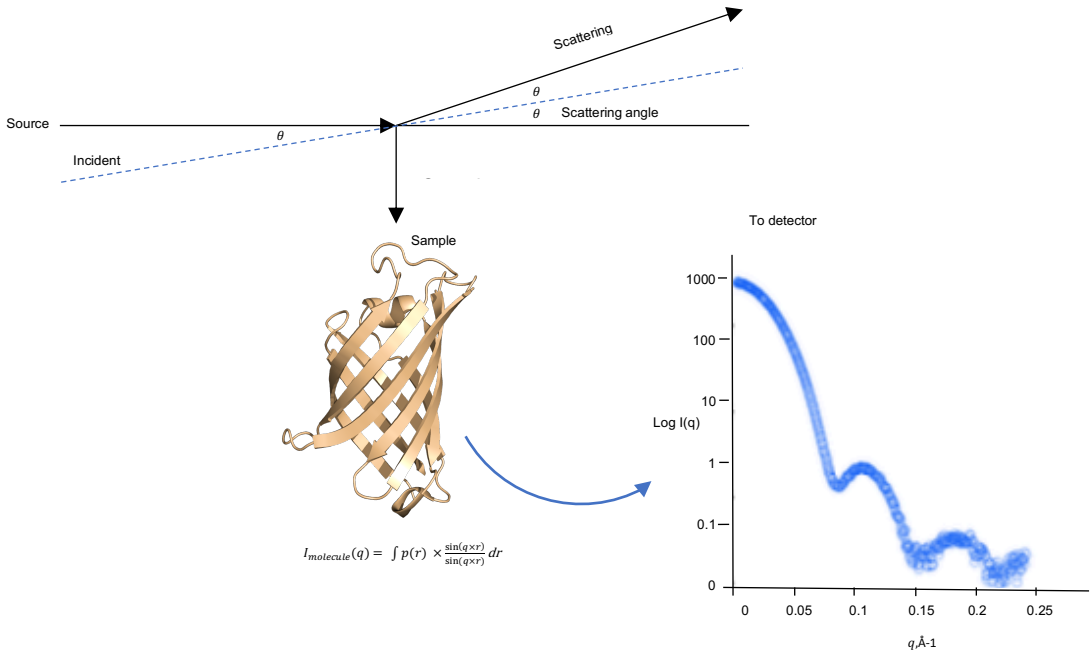

Figure 3.12 Calculation of protein structure using SAXS. Using the p(r) function, which encompases a set of all distance vectors within the molecule, relating scatter intensity (I) to q (the scattering vector). The data at small values of q correlates to large distance vectors within the particles. The separate peaks indicate a poly-dispersed sample, with higher molecular weight populations seen at lower q values, given in inverse angstroms ($Å^{-1}$). The graph was generated using the program ScÅtter.

The radius of gyration (Rg) measured in reciprocal space is called the Guinier fit and describes the distribution of mass around a particle's centre of inertia. A Guinier analysis produces a straight line that slopes downwards; where Rg is the slope of that line. There is an approximation in which a globular particle will show a straight-line relationship in the low q region, which was observed for both native AbyU and [C-AbyU][S] (Figure 3.13). The normal distribution of the residuals along the straight line for [N-AbyU] and [C-AbyU][S] indicate that the protein is behaving as expected, and shows that the calculated fit is good, allowing accurate calculation of SAXS parameters. A deviation from linearity is indicative of protein aggregation.

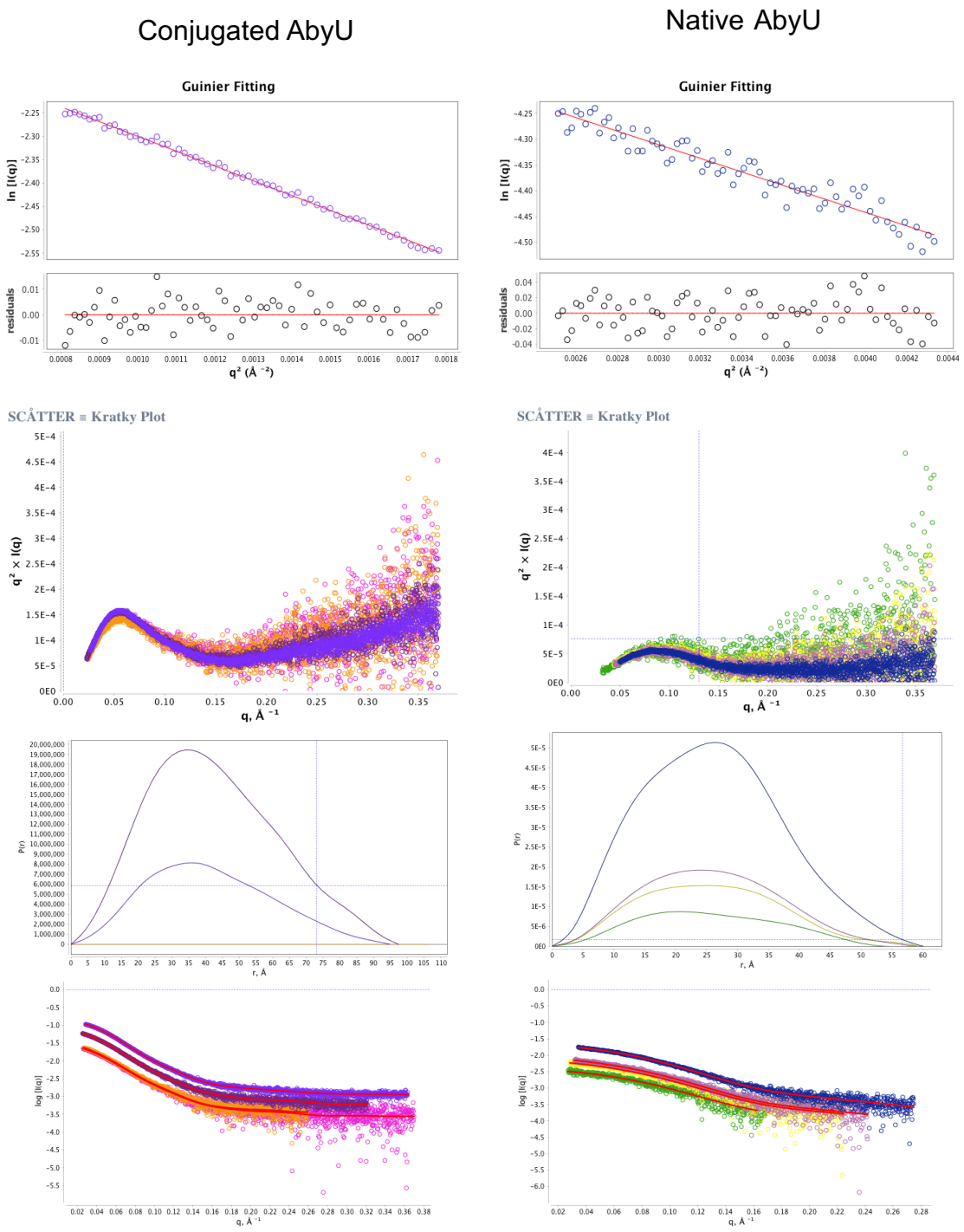

Figure 3.13 Guinier linear approximation and Kratky plots used to assess structure and size of [N-AbyU] and [C-AbyU][S]. The Guinier fitting of the raw data is plotted as q^2 $Å^{-2}$ vs. the scattering intensity (ln[I(q)]). The red lines indicate the trendline, the individual data points from the beamline are represented as circles. Convergence of the p(r) function to the x axis in the Kratky plot indicates the extent of folded protein. Buffer subtraction was carried out to determine the scattering effect from the particles only. Data fitted by Carl Marsh using the program ScÅtter.

Protein folding was analysed using Kratky plots, which were generated from the p(r) function. The function exhibited a bell-shaped peak at low q for [N-AbyU] and [C-AbyU][S], that converged smoothly to the x axis, signifying well-folded, globular protein (Figure 3.13). Significantly, the plot will not approach the q axis if the protein has pronounced flexibility or if it is unfolded (Figure 3.14). Interestingly, the native enzyme appears to converge at a lower q value and has less features of a flexible protein. A reason for this could be that the surfactant has introduced non-native flexibility to the protein, by creating new contacts to and around the protein structure. The extended tails, observed as a departure from the q axis and a lack of fit of the residuals observed in the (log [I(q)]) vs. q plot, suggest that there is a large object adversely affecting the data, which is possibly caused by the formation of AbyU tetramers. This could be a valid explanation as the NATIVE-PAGE analysis of native AbyU found that the enzyme forms tetramers in solution (as demonstrated later in Figure 3.15).

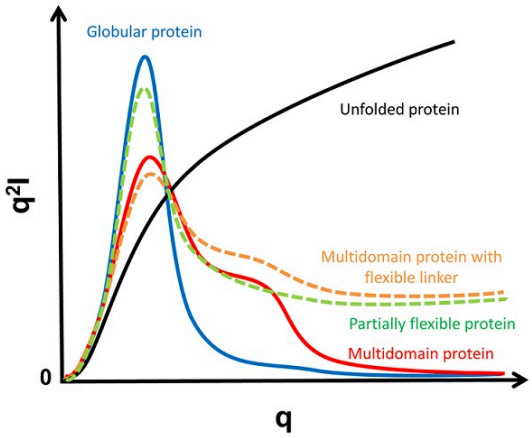

Figure 3.14 Kratky plot analysis, which informs on protein globularity and flexibility. Taken from (Stanford, 2017).

The p(r) function estimates the particle volume (given in cubic angstroms) and the dmax, which is the maximum dimension of the particles. Since the [N-AbyU] and [C-AbyU][S] samples are polydispersed, these calculated values are a mean average of the ensemble of particles in the sample, therefore this can generate a 'fuzzy cloud' density, which is likely to be much bigger than the actual MW (Stanford, 2017), and give a larger volume than would be expected. This could account for the large MW and total volume for the protein samples reported by the analysis. [C-AbyU][S] was approximately 4x the volume of the native protein (Table 3.2), which indicates

successful surfactant conjugation, as this would account for the greater dimensions of [C-AbyU][S] compared to [N-AbyU]. The polymer surfactant IGEPAL-890 (MW ~1,982 Da) is expected to conjugate to the 37 basic residue sites on AbyU, which will result in a molecular weight of ~ 91, 074 Da (= 37 × 1,982 + 17, 700), assuming 100% conjugation efficiency. This is similar to the molecular weight increase reported by the SAXS analysis (Table 3.2), and provides evidence for the addition of 37 surfactant molecules to the basic residues of AbyU.

	Conjugated AbyU	**Native AbyU**
Rg (radius of gyration, Å)	30.7 (31.89)	19.5 (20.08)
Dmax (maximum dimension, Å)	98	67.5
Volume ($Å^3$)	~160,000	~42,000
Molecular Weight (Da)	~100, 548	~30,687

Table 3.2 Summary of SAXS parameters. The dmax is the longest distance in the particle, it is derived from the p(r) function estimates the fit of the data to the p(r) function. The approximate molecular weight of the particles is calculated by diving the volume (given in cubic Å) from the straight-line plateau by the density of protein (an approximation of 1.7).

Additional evidence was obtained from NATIVE-PAGE analysis of the protein samples under investigation. Samples were loaded side by side to aid discrimination between modified and unmodified samples (Figure 3.15). [C-AbyU][S] yielded a spectrum of species of different masses, suggesting that the protein-polymer had aggregated to give a range of species. This may indicate surfactant ‘stickiness’. In contrast,

unmodified his-tagged native AbyU migrated with a mass equivalent to 66 kDa, an apparent molecular mass of a quaternary species (a dimer of dimers). No monomeric (tagged MW ~17 kDa) AbyU was detected on the gels. This suggests that stable AbyU dimers associate in solution to form tetramers. These results provide further indication that the conjugated enzyme is greater in molecular weight than the native.

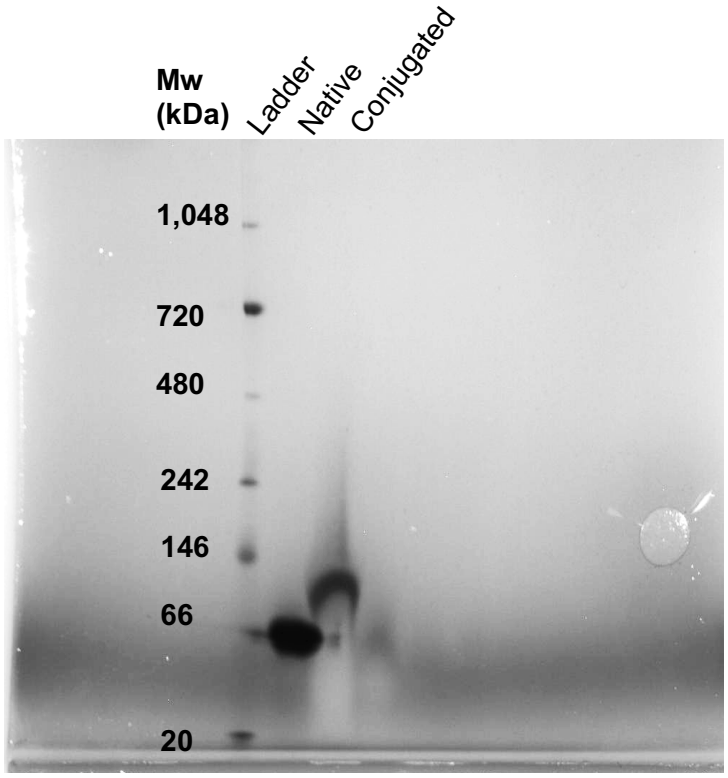

Figure 3.15 NATIVE-PAGE analysis of purified AbyU samples. The AbyU preparations were diluted to 1 mg. mL^{-1} to achieve appropriate protein loads to visualise the bands. A NativeMark Unstained Protein Standard (ThermoFisher) molecular weight marker was used. Electrophoresis employed 8% polyacrylamide gels. Samples were visualised using Coomassie blue staining. The asterisk indicates the migration position of the native His-tagged AbyU, which was ~66 kDa and is roughly the size of an AbyU tetramer.

The NATIVE-PAGE results are in agreement with the SAXS analysis and are compelling evidence that protein modification has successfully yielded protein-polymer bioconjugates. Following verification of successful conjugation, characterisation of the modified AbyU enzyme was performed and benchmarked against unmodified native AbyU, to determine the effects of modification on enzyme function.

3.6 Determining Stoichiometry of Surfactant Conjugation

A standard curve of surfactant absorption was produced in order to estimate the extinction coefficient of the surfactant (Figure 3.16). The absorbance was measured spectrophotometrically at 280 nm.

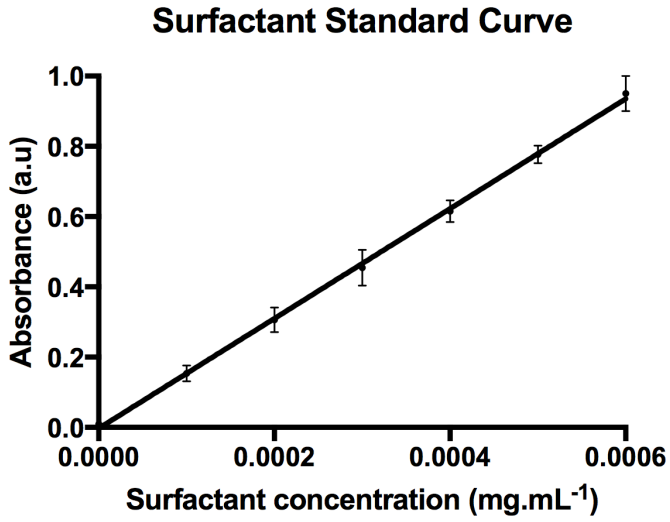

Figure 3.16 Standard curve used to estimate molar absorption coefficient (ε) of the surfactant. The absorbance was measured at 280 nm at different concentrations of surfactant. Using the Beer-Lambert law (equation 1), the gradient of the straight line enables estimation the molar absorption extinction coefficient of the surfactant. In this case, ε = 1595.1 $L.mol^{-1}cm^{-1}$.

The stoichiometry of surfactant conjugation was determined using an equation of the form:

$$Abs_{280}[AbyU_{Surf}] = Abs_{280}[AbyU_{Native}] + Abs_{280}[Surfactant]$$

A 0.1 $mg.mL^{-1}$ sample of [C-AbyU][S] absorbed 0.78 units at 280 nm (Figure 3.17). A 0.1 $mg.mL^{-1}$ sample of native protein absorbed 0.23 units at 280 nm.

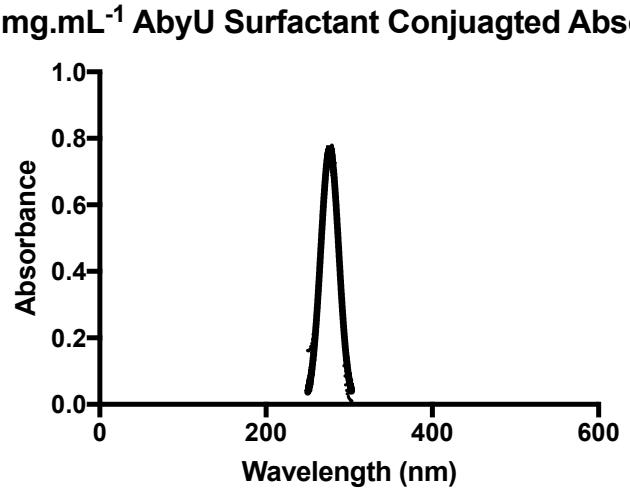

Figure 3.17 Absorption spectra of [C-AbyU][S] over the wavelength range 0 – 600 nm. A peak is visible at 280 nm. This absorbance value was used to determine $Abs_{280}[AbyU_{Surf}]$.

Following the equation; 0.78 = 0.23 + x

$x = 0.55$

Inputting the calculated absorbance value into the Beer-Lambert equation to solve for the concentration of surfactant, c = $\frac{A}{\varepsilon L}$

c = $\frac{0.55}{1595.1 \times 1}$ = 3.44×10^{-4} mol.L^{-1}

Moles of surfactant = 3.44×10^{-4} mol.L^{-1} × 100 μL = $3.44\ 10^{-8}$ mol

Moles of AbyU = $\frac{(0.1\ mg.mL \times 100\ \mu L)}{17740\ g.mol^{-1}}$ = 5.6×10^{-10} mol

Moles of surfactant added per mole of AbyU = $\frac{3.4 \times 10^{-8}\ \text{mol}}{5.6 \times 10^{-10}\ \text{mol}}$ = 60

This shows that for every mole of AbyU, 60 surfactant chains are conjugated to the protein.

3.7 Chemical Denaturation Studies to Evaluate Enzyme Tolerance

Unfolding characterisation of AbyU in 'harsh' reaction conditions were performed to assess enzyme tolerance and catalytic performance. The native enzyme was irreversibly unfolded using the denaturant guanidinium hydrochloride (GuHCl) in order to generate a reference of attributes for comparison with the modified enzyme. The tertiary structure composition of AbyU as a function of denaturant concentration was monitored using fluorescence spectroscopy. This technique exploits the intrinsic fluorescence of the tryptophan residues in AbyU. Protein stability was found to correlate with denaturant concentration (Figures 3.18 – 3.20).

A **Unfolding of Native AbyU Using Increasing [GuHCl]**

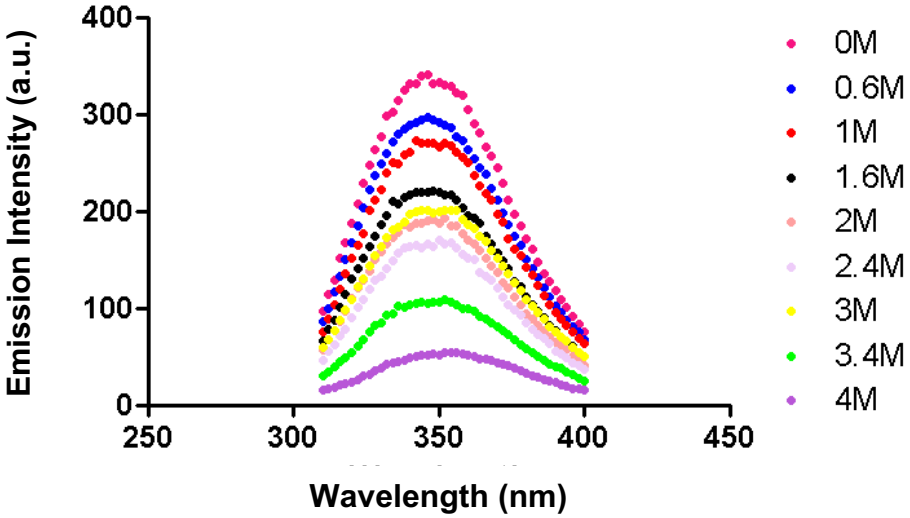

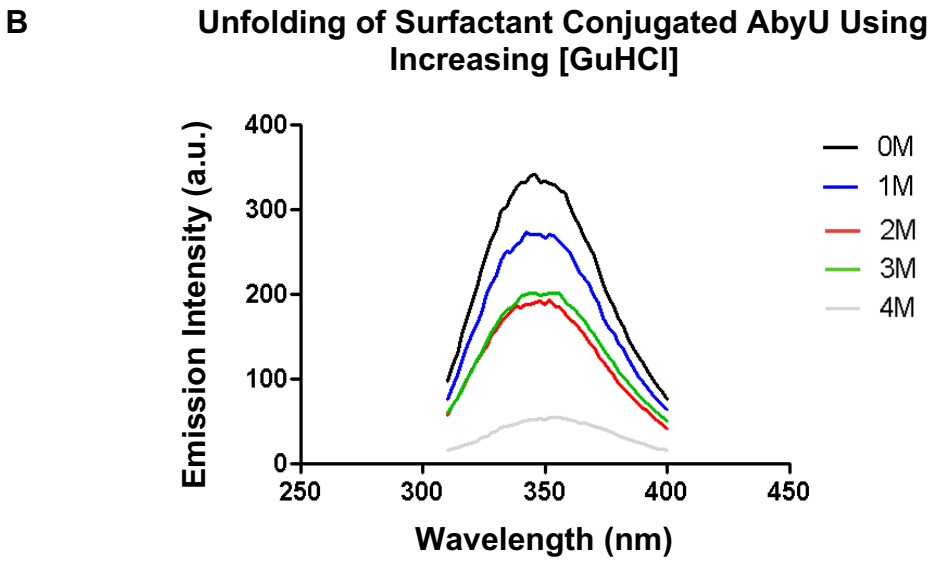

Figure 3.18 Emission spectra of (A) Native and (B) Conjugated AbyU in the presence of up to 4 M GuHCl denaturant. Scans were taken across the wavelengths 300 nm – 400 nm. Each protein exhibited a well-defined peak ~350 nm. This is due to the tryptophan fluorescence signal, a decrease in which corresponds to a loss of protein secondary structure.

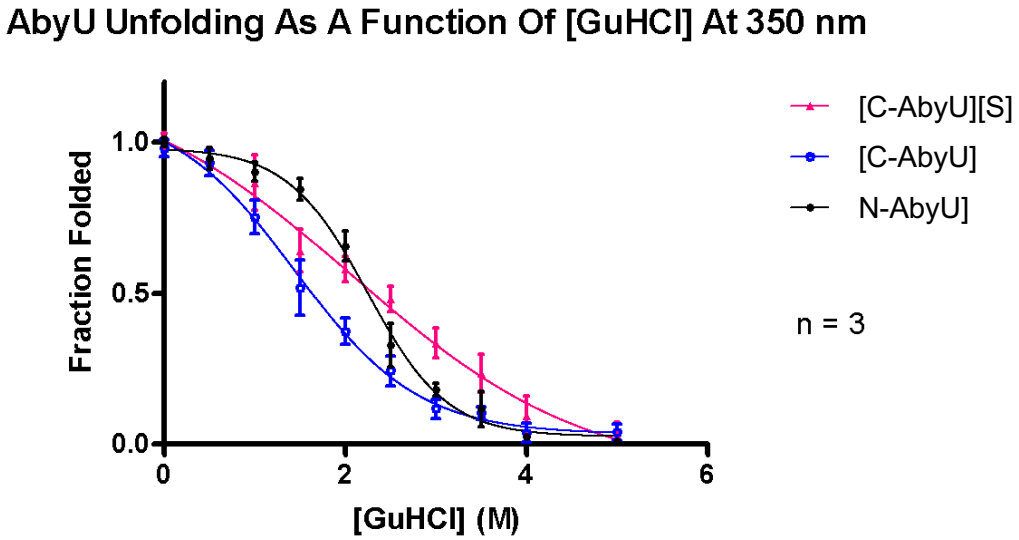

Figure 3.19 Chemical unfolding profiles of [N-AbyU], [C-AbyU] and [C-AbyU][S] in GuHCl.

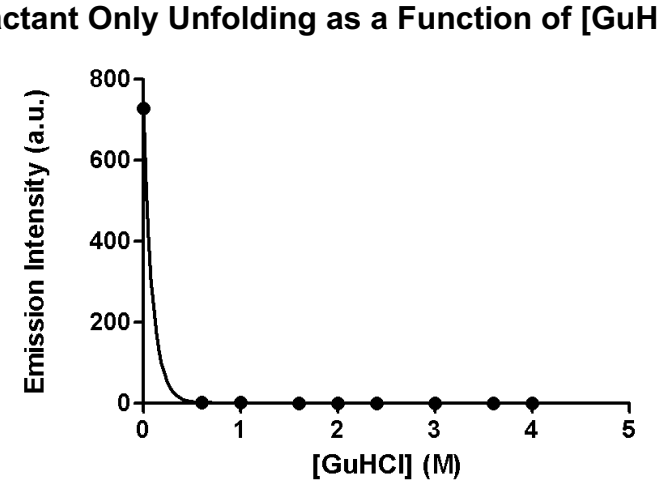

Figure 3.20 Spectroscopic scan of surfactant emission at 350 nm. This was background subtracted from the emission spectra of [C-AbyU][S].

Native AbyU was found to retain tertiary structure in the presence of denaturant at concentrations up to 3 M (Figure 3.18). GuHCl-induced unfolding shows a cooperative transition of the native protein and reveals that the protein unfolds *via* a two-state (native ↔ unfolded) mechanism. Conjugated AbyU exhibits an increased tolerance to higher concentrations of denaturant. This could be explained by the addition of the surfactant corona, which may physically protect the protein from exposure to denaturant. Together, this could account for the non-cooperative behaviour exhibited by [C-AbyU][S], as the surfactant corona may be acting to maintain protein structure, until a critical proportion of native contacts are lost. [C-AbyU] is rapidly unfolded at lower concentrations (2 M) of denaturant (Figure 3.19). This could be due to a change in the charge of the side groups, or due to the non-catastrophic conformational changes made to the enzyme's β-barrel structure during the process of cationisation that has left the tryptophan residues, normally protected on the inside of the protein, exposed to denaturant. This may be evaluated by performing the experiment in the presence of tryptophan only. However, it should be noted that tryptophan (W) is not an ideal reporter as its fluorescence signal changes upon solvent exposure. For these reasons, it was necessary to carry out further enzyme characterisation, as is detailed below.

3.8 Circular Dichroism Spectroscopy

A number of spectroscopic and binding studies were performed in an effort to investigate the structure and function of modified AbyU polypeptides. The thermal unfolding behaviour of AbyU was examined using circular dichroism (CD) spectroscopy, a technique that reports on protein secondary structure (far-UV CD 200-250 nm) and tertiary structure (near-UV CD 260-300 nm). CD analyses revealed that the introduced chemical modifications had minimal impact on the secondary and tertiary structure of AbyU at 25 °C, with peaks in the CD spectra characteristic of a predominantly β-structure observed (Figure 3.21). The far-UV CD spectrum of AbyU reveals a minima at ~220 nm, which is typical of proteins with high beta-strand content, and in keeping with the X-ray structure of the enzyme.

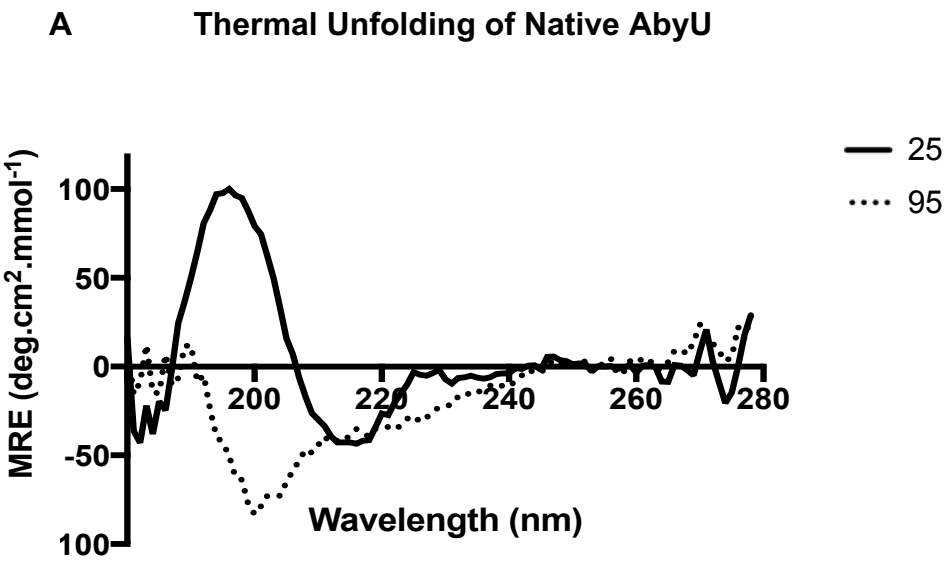

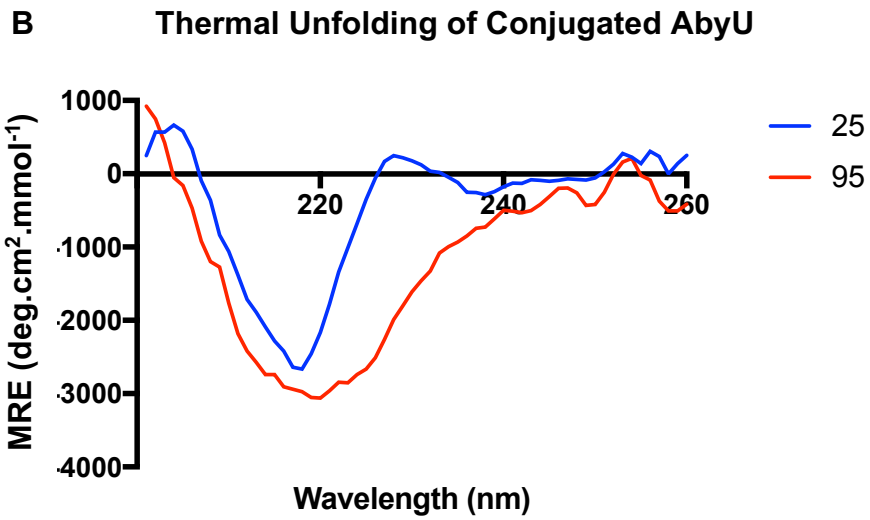

Figure 3.21 Structural characterisation of the protein complexes. CD spectroscopy was used to analyse the structure of native AbyU and [C-AbyU][S]. **(A)** Near-UV CD of [N-AbyU] and **(B)** near-UV CD of [C-AbyU][S] in molar residue ellipticies (MRE). Superimposed traces indicate retention of native secondary and tertiary structure, at 25°C (blue trace) and a loss of β-barrel structure at ~225 nm at 95°C (red trace). The peaks observed at 180 nm were present in both samples, indicating that the conjugated enzyme retained the predominantly β-barrel secondary structure of native AbyU.

Thermal denaturation of AbyU reveals no loss in secondary structure at temperatures up to 65 °C. Above this threshold, however, the enzyme undergoes a rapid, non-reversible, unfolding. This was confirmed by carrying out thermal refolding experiments on native and conjugated AbyU, incrementally decreasing the temperature from 95 °C to 25 °C. Neither enzyme recovered the folded state after heating to 95 °C (Figure 3.22).

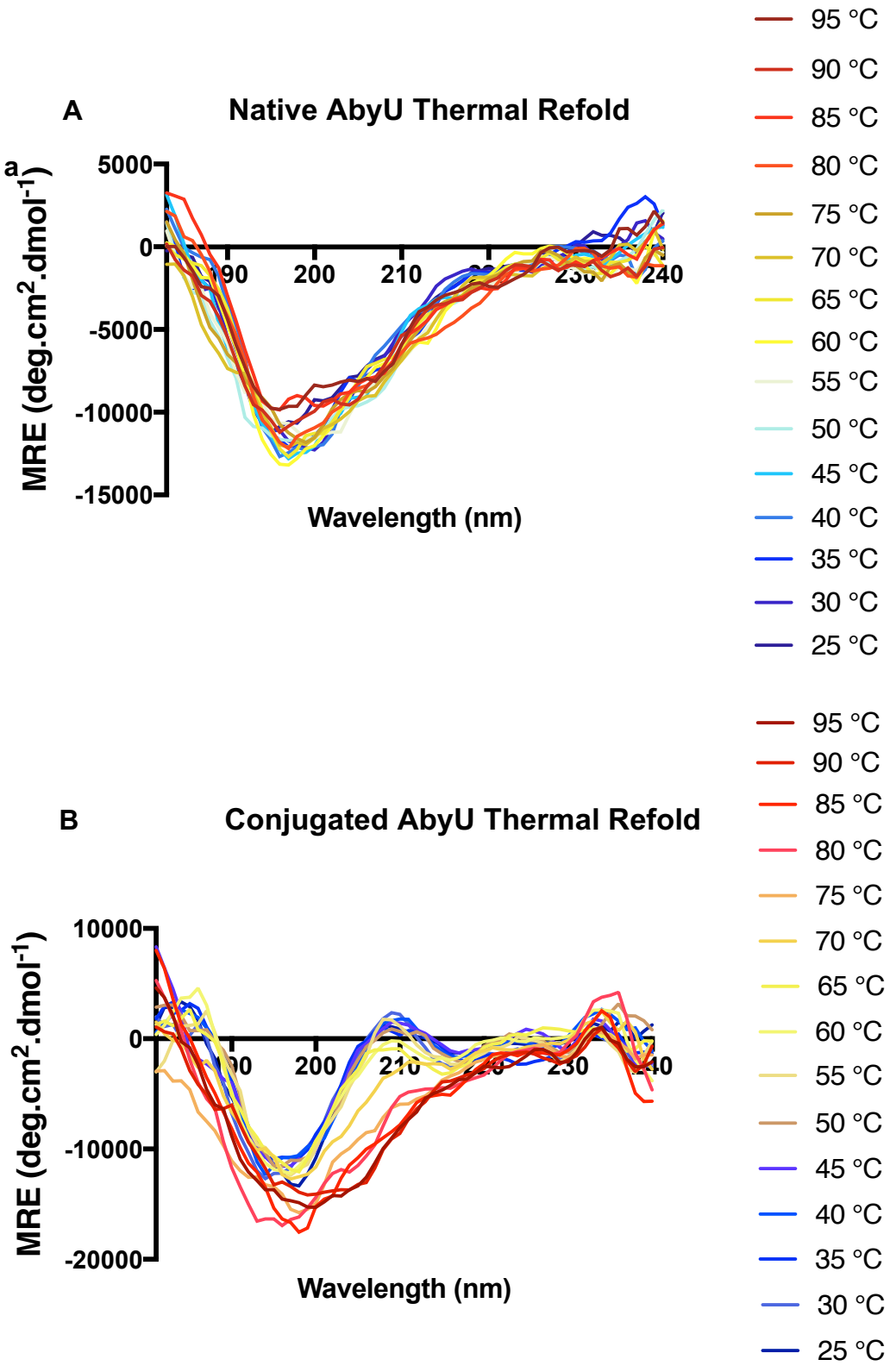

Figure 3.22 Structural characterisation of thermally refolded AbyU. Far-UV CD was used to analyse protein secondary structure of **(A)** N-AbyU] and **(B)** [C-AbyU][S] upon cooling back down to 25 °C. No refolding was seen after heating to 95 °C in either the native or conjugated samples. The blue trace indicates 25°C and the red trace 95°C.

Thermal denaturation melting curves (λ=220 nm) showed progressive decreases in stabilities (Figure 3.23). [C-AbyU][S] exhibited a half denaturation temperature of 70 °C, compared with 62 °C for [N-AbyU]. This represents a modest increase in thermal stability due to conjugation and suggests that modification has improved the structural stability of the enzyme at higher temperatures. A reason for this could be that the surfactant corona has increased the stability of amino acid contacts within the barrel, and this has made the structure more resistant to heating.

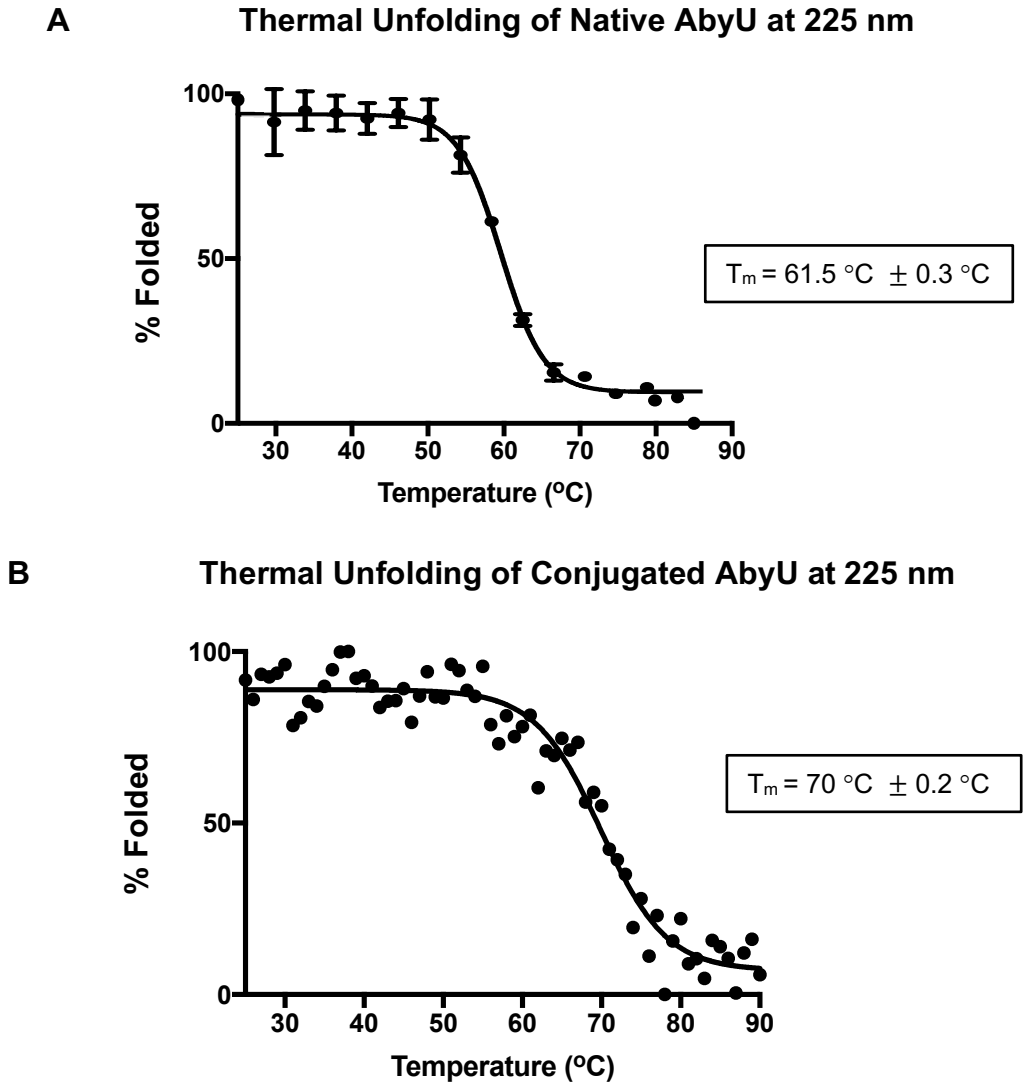

Figure 3.23 Temperature denaturation profiles of AbyU. (A) [N-AbyU] and **(B)** [C-AbyU][S] plots were fitted to sigmoidal curves (black lines). The half denaturation temperature of native AbyU and conjugated AbyU were calculated to be 61.5 °C and 70°C, respectively.

3.9 Enzyme Activity Assays

To complement folding studies of native and modified AbyU, the catalytic activity of these proteins was investigated. This was achieved initially by monitoring the conversion of a diketone synthetic analogue of AbyU's natural substrate to its spiro-cyclic product by LCMS as previously reported (Figure 3.24; Byrne et al., 2016). AbyU accepts a synthesised OMe-substituted substrate analogue and converts it to the corresponding product. The methyl group protects the substrate, to an extent, from auto-cyclisation. Enzyme independent cyclisation of this compound was detected. As a consequence, this background reaction was subtracted from all readings. This rate was calculated to be 0.01 ± 0.002 min^{-1}.

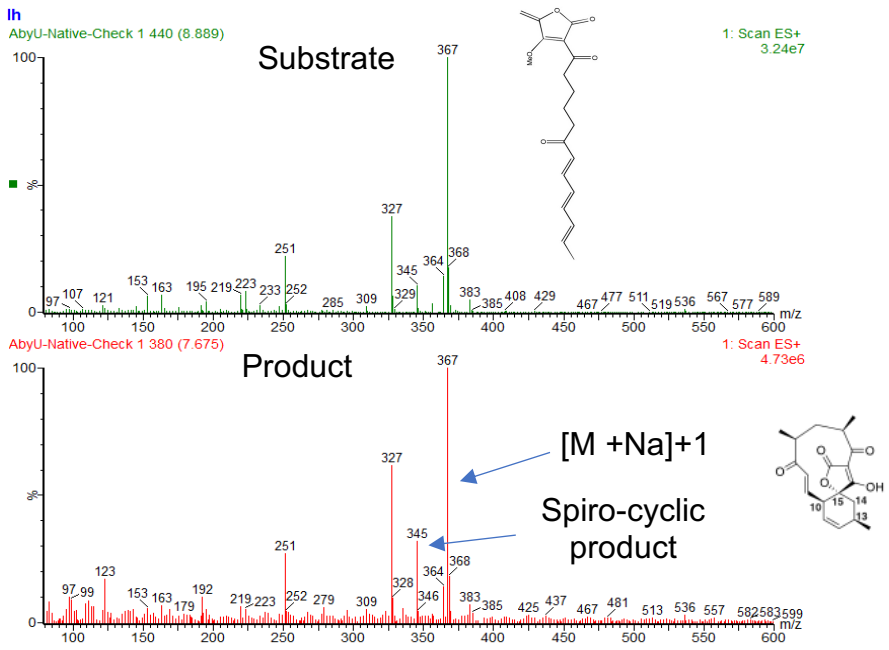

Figure 3.24 Mass spectra of AbyU substrate and AbyU catalysed reaction products. Positive ion mode ESI MS of the substrate and product, recovered from AbyU catalyzed [4+2] cycloaddition reactions. Product masses are consistent with the structure with *m/z* of $[M + Na]^+$ = 367.53 (theoretically predicted: 367.15).

LC-MS based assays, that involved the quantitation of the spiro-cyclic reaction product, were used to determine the relative activities of native and modified AbyU (Figure 3.26). Comparative analysis of the results demonstrated that the enzyme-catalysed substrate turnover rates were faster than that of substrate alone. Surprisingly, the rates of [C-AbyU] and [C-AbyU][S] were faster than for the native enzyme. These data give compelling support for an enhancement in the rate of AbyU catalysed [4+2] cycloaddition when the enzyme has undergone modification, an observation that warranted further investigation.

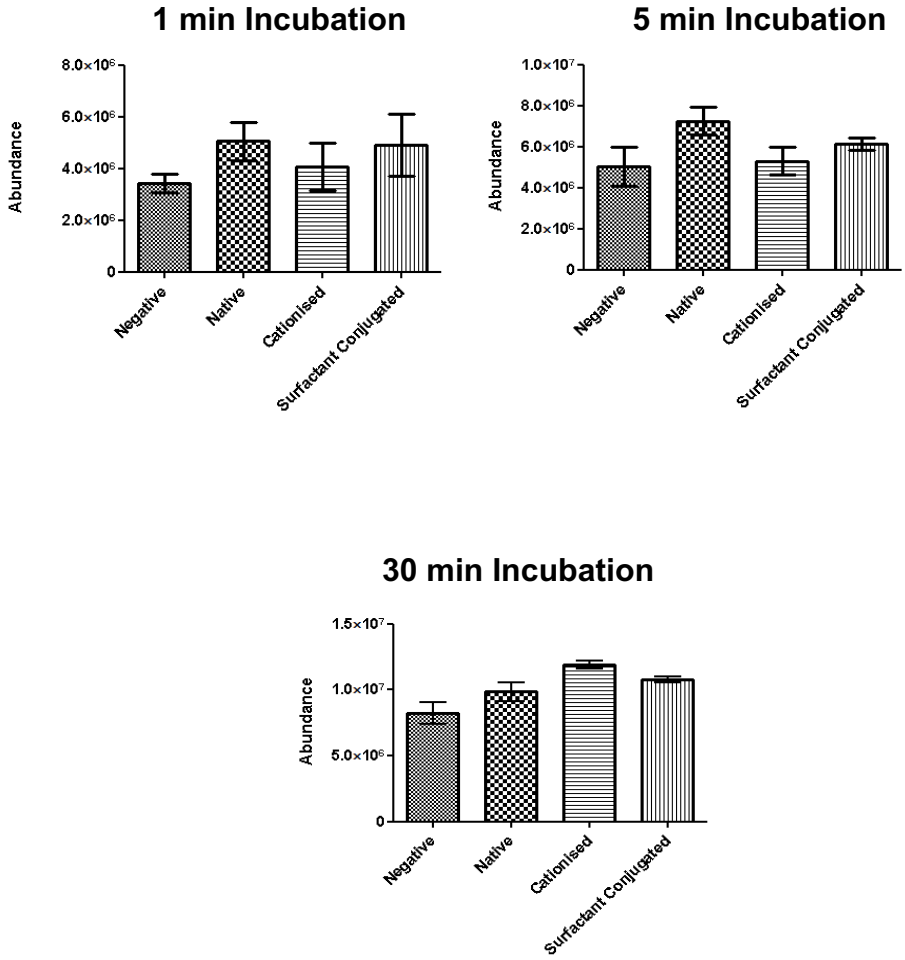

Figure 3.25 Native and modified AbyU activity assays. LC-MS assays measuring rate of disappearance of substrate at 325 nm after 1 min, 5 min or 30 min incubations with AbyU. 10 mM substrate was incubated in the presence or absence of 280 μM AbyU at 25 °C. The error bars are mean average and standard deviations based on abundance of substrate at 325 nm from 3 separate reactions.

3.10 Elucidation of Enzyme Reaction Rates

To determine the effects of modification on enzyme catalytic activity, initial velocities of the AbyU catalysed and non-catalysed reactions were measured spectrophotometrically at 325 nm. Conjugated enzyme turnover rates were found to be significantly faster than for the native enzyme, suggesting that modification had improved catalytic performance (Figure 3.27).

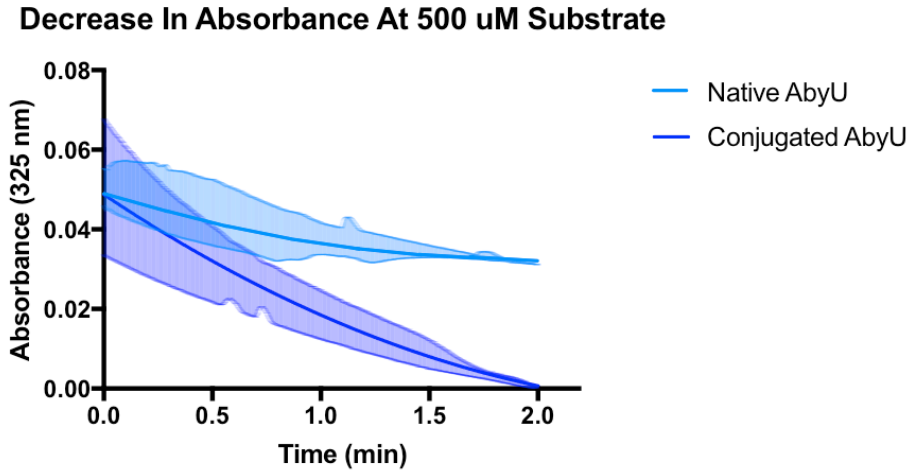

Figure 3.26 The rate of substrate disappearance at 325 nm catalysed by [N-AbyU] and [C-AbyU][S]. Measurements were taken at 0.01 min intervals during the reactions and fitted to a standard exponential decay. The bold lines indicate the trendline, and lighter shaded areas indicate error bars (standard errors of the mean), averaged from *n*=3.

Next, a complete steady state kinetic characterisation was performed (Figure 3.28 and Table 3.3). Substrate turnover per enzyme active site is increased following cationisation and conjugation, as is indicated by enhancements in k_{cat}. An increase in K_m is also observed, which could be explained by the attachment of surfactant polymer to the capping loop of the enzyme, as exemplified by the high proportion of cationised sites in this area. This could preclude substrate from entering and exiting the catalytic site. This would decrease enzyme affinity for the substrate and the enzyme would require a higher concentration of substrate to achieve maximum turnover rate (Berg, Tymoczko, & Stryer, 2002). Unfolded conjugated and unfolded native enzymes were

found to have activities equivalent to substrate only, whilst the active samples of modified enzyme are unequivocally higher.

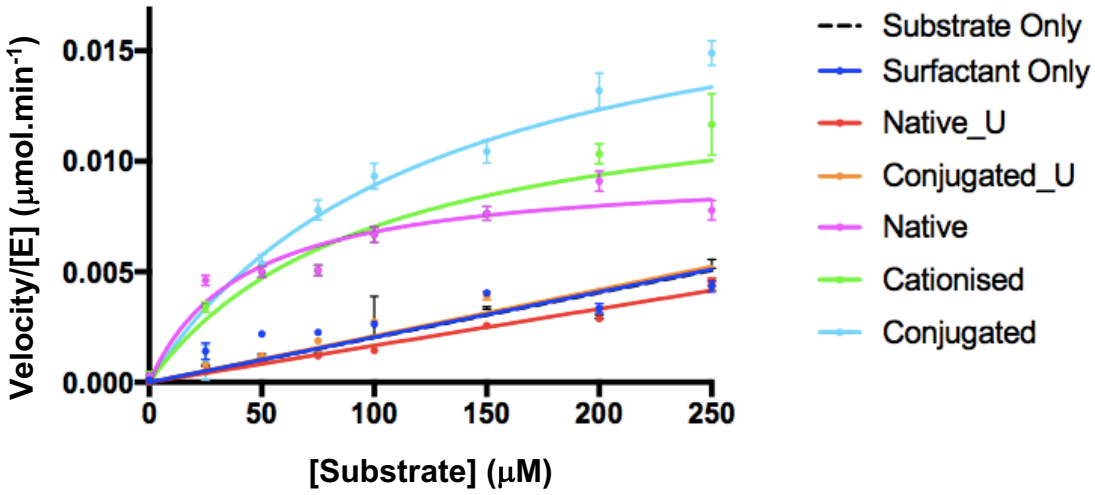

Figure 3.27. Kinetic analysis of non-enzymatically catalysed and enzymatically catalysed reactions, at varying concentrations of substrate. Substrate turnover was monitored spectrophotometrically at 325 nm. Results were obtained in triplicate and the standard error from the mean calculated. The difference in rate between the enzyme catalysed and uncatalysed reactions were analysed.

	[N-AbyU]	[C-AbyU]	[C-AbyU][S]
K_m (μM)	41 ± 15	99 ± 19	124 ± 22
k_{cat} (min^{-1})	357 ± 40	420 ± 31	751 ± 72
k_{cat}/K_m (μM. min^{-1})	8.5 ± 1.5	4.2 ± 0.8	6.0 ± 1.2

Table 3.3 Calculated kinetic parameters for native and modified AbyU.

Chapter 4. Discussion

In this study, a protein modification technique has been applied to the natural Diels-Alderase AbyU. It was hoped that this method could be used to improve the tolerance of the enzyme to 'harsh' reaction conditions and hence improve its suitability for use in industrial processes. The work presented herein demonstrates the tractability of this approach and lays the groundwork for its future application to other enzyme targets. AbyU was found to be highly amenable to bioconjugation and satisfactory yields of modified enzyme conjugates could be recovered. Total loss of protein structural integrity following bioconjugation is common, as the harshness of the process may initiate enzyme unfolding. This is an often-reported negative consequence of protein modification by cationisation and surfactant conjugation. A 24-hour incubation at pH 6.0 typically with high titres of DMPA and EDC will effectively 'attack' the protein target, causing polypeptide destabilisation and aggregation. Some optimisation of conjugation conditions was required during this study, however, this was to be expected given the invasive nature of the technique.

Analytical methods were successfully applied to elucidate the degree and location of modifications on the enzyme, revealing that these were restricted to acidic residues located in the loop regions of AbyU and the outer surface of the protein. No conjugation was observed for residues that reside within the enzyme active site, which gave encouragement that AbyU may retain catalytic activity following treatment.

Circular dichroism and fluorescence spectroscopy have been applied to examine the secondary structure composition of the modified polypeptides and their susceptibility to thermal and chemical denaturation as compared to native AbyU. These studies found that surfactant conjugated [C-AbyU][S] was the most stable form of the enzyme, with an improved tolerance to high temperature and denaturants. Native AbyU has a T_m of 61.5 °C $\pm$ 0.3 °C and a GuHCl denaturation midpoint of 2 M, whereas conjugated AbyU has a T_m of 70 °C $\pm$ 0.2 °C and a GuHCl denaturation midpoint of 3 M. This could be suggestive that the modification process has conferred enhanced stability to the enzyme, as the surfactant may be reinforcing the structural integrity of the protein structure. The improvements in stability of AbyU were modest, though

significant, as the degree of enhancement in protein stability will be target dependent. Proteins with a higher percentage of modifiable amino acids will be subject to greater conjugation and consequently may exhibit better improvements in their tolerance to denaturants and high temperature.

Kinetic characterisation of AbyU conjugates demonstrated that these modified enzymes retain catalytic function, though exhibit significant changes in their steady-state kinetic parameters. This is perhaps unsurprising given the size and extent of the modifications that have been performed. MALDI-MS studies demonstrated the presence of modifications in the active site capping loop of AbyU. The flexibility of this loop is known to be of importance in mediating substrate entry and product exit from the enzyme active site. Conjugation in this region is likely to have significant impact on catalysis and may account for the observed changes in kinetic parameters. For example, should the flexibility of this loop be impaired, or access to the active site restricted, this may limit the catalytic competency of the enzyme. There are also potential effects arising from distal conformational changes within the barrel fold of AbyU resulting from bioconjugation that may influence the conformational dynamics of the enzyme.

The introduction of the conjugate corona around the enzyme may also have an effect on the attraction or repulsion of substrate molecules. This will have an impact on substrate availability to the enzyme active site. The increased K_m observed for AbyU bioconjugates implies that the enzyme has a reduced affinity for substrate. This would be consistent with the largely hydrophobic substrate interacting with the hydrophobic tails of the surfactant, reducing the rate of transfer to the enzyme active site. Therefore, it seems that, although improvements to K_{cat} were observed, the concomitant increase in K_m suggests that the overall enzyme kinetics of the conjugated protein has remained similar to that of the native. Suggesting that conjugation may not confer enhanced enzyme kinetics, but that it does not impair them either, as might be expected following harsh modification processes.

The SAXS analyses reported herein suggest that conjugation results in a significant enhancement in the hydrodynamic radius of AbyU. Whilst this does show that the

enzyme has increased in mass and is encouraging to the hypothesis that the protein has undergone modification, it is difficult to be certain whether conjugation to the desired surfactant polymer has been undoubtedly successful without more detailed structural information about the nature of the polymer corona.

Conjugated variants of AbyU showed no reduction in solubility in aqueous solvent. This was unexpected, given the hydrophobic nature of the polymer surfactant used, however, similar results have been reported by others who have generated equivalent conjugates of eGPF (Armstrong et al., 2015). Both AbyU and eGFP are inherently stable proteins with high solubilities. The latent physio-chemical properties of the conjugated target proteins may be a factor in ensuring compatibility with aqueous systems and this could be readily tested by applying our conjugation method to inherently less stable polypeptides.

The benefits of the process outlined in this thesis are that it creates proteins with advantageous properties, such as retained catalytic activity and modestly improved thermal stability without any requirement to alter the primary amino acid sequence of the target protein. For this reason, the approach may have wide-ranging use in the modulation of protein function and specifically as a method to improve the compatibility of proteins with non-aqueous based solvent systems. In a complimentary study conducted in Bristol (Marsh et al., unpublished) it was shown that this treatment significantly improved the kinetic behaviour of AbyU for its cognate substrate in organic solvent systems, such as those commonly employed in process chemistry. Exploration of the solvent preferences of AbyU conjugates is a major focus for future research activity. Another future direction that will be explored is optimisation of surfactant choice. This will involve kinetic analysis of AbyU conjugated to different polymers and studying the resultant catalytic effects. Different surfactants may define enzyme function in different solvent systems, which will in turn greatly influence key aspects of protein stability and folding, resulting in thermodynamic and kinetic effects.

The conjugated enzyme is highly heterogeneous due to the dynamic nature of the corona. However, valuable structural information could be acquired using techniques that are tolerant of dynamic protein systems. Elucidation of an NMR structure of AbyU

is almost complete and consequently this may be the favoured method for structural characterisation of AbyU polymer conjugates in the future.

Chapter 5. Acknowledgements

I would like to thank Paul Race, Steven Burston, Carl Marsh, Laurence Maschio, Alice Pernell, Kate Heesom and Li-Chen Han for their help and support throughout this project. I would also like to thank the C101 group.

Chapter 6. References

Armstrong, J., Rameen, S., Horne, J., Dickinson, S., Armstrong, C., Perriman, A., Lowe, R. (2015). Artificial membrane-binding proteins stimulate oxygenation of stem cells during engineering of large cartilage tissue. *Nature Communications,* (6), 7405.

Beifuss, U., Tietze, L. (1993). Sequential Transformations in Organic Chemistry: A Synthetic Strategy with a Future. *Angewandte Chemie, 32* (2), 131−163.

Berg, J., Tymoczko, J., Stryer, L. (2002). The Michaelis-Menten Model Accounts for the Kinetic Properties of Many Enzymes. *Biochemistry 5th edition.* (Section 8.4). New York: W H Freeman.

Brogan, A., Hallet, J. (2016). Solubilizing and Stabilizing Proteins in Anhydrous Ionic Liquids through Formation of Protein−Polymer Surfactant Nanoconstructs. *Journal of the American Chemical Society, 138* (1), 4494−4501.

Brogan, A., Sharma, K., Perriman, A., Mann, S. (2013). Isolation of a Highly Reactive β-Sheet-Rich Intermediate of Lysozyme in a Solvent-Free Liquid Phase. *Journal Of Physical Chemistry, 117* (28), 8400−8407.

Byrne, M., Lees, N., Han, L., van Der Kamp, M., Mulholland, A., Stach, J., Race, P. (2016). The Catalytic Mechanism Of A Natural Diels-Alderase Revealed in Molecular Detail. *Journal of the American Chemical Society*, *138* (19), 6095-6098.

Chakraborty, S., Rusli, H., Nath, A., Sikder, J., Bhattacharjee, C., Curcio, S., Drioli, E. (2016). Immobilized biocatalytic process development and potential application in membrane separation: a review. *Critical Review Biotechnology, 36* (1), 43-58.

Chandra Mohanaa, N., Yashavantha Raoa, H., Rakshitha, D., Mithunb, P., Nuthana, B., & Satish, S. (2018). Taking nature's enzymes and modifying them, for example through directed evolution or genetic approaches, represent a leading way for mining for new antibiotics in this era. *Journal of Genetic Engineering and Biotechnology, 16* (1), 1-8.

Cyclic Dienes and Dienophiles in the Diels-Alder Reaction (2019). *Master Organic Chemistry.* Retrieved May 8, 2019, from [online]. Available at:

https://www.masterorganicchemistry.com/2017/09/08/cyclic-dienes-and-dienophiles-in-the-diels-alder-reaction/

Choi, J., Han, S., Kim, H. (2015). Industrial applications of enzyme biocatalysis: Current status and future aspects. *Biotechnology Advances, 33* (7), 1443-1454.

Correia Carreira, S., Armstrong, J. P., Okuda, M., Seddon, A. M., Perriman, A. W., & Schwarzacher, W. (2016). Synthesis of Cationized Magnetoferritin for Ultra-fast Magnetization of Cells. *Journal of visualized experiments,* (118).

de Regil, R., Sandoval, G. (2013). Biocatalysis for Biobased Chemicals. *Biomolecules, 3* (4), 812–847.

Dias, D., Urban, S., Roessner, U. (2012). A Historical Overview of Natural Products in Drug Discovery. *Metabolites, 2* (2), 303–336.

Extance, A. (2016). Active esters enable powerful new route to carbon–carbon bonds. *The Royal Society Of Chemistry*. Retrieved March 14, 2018, from [online]. Available at: https://www.chemistryworld.com/news/active-esters-enable-powerful-new-route-to-carbon-carbon-bonds-/1010314.article

Farkaš, P., Bystrický, S. (2010). Chemical conjugation of biomacromolecules: A mini-review. *Chemical Papers, 64* (6), 683–695 .

Fesko, K., Gruber-Khadjawi, M. (2013). Biocatalytic Methods for C–C Bond Formation. *Chem Cat Chem Reviews*, 5 (6), 1248–1272.

Laage, D., Elsaesser, T., Hynes, JT. (2017). Water Dynamics in the Hydration Shells of Biomolecules. *Chemical Reviews*, *117* (16), 10694–10725.

Francis, O., Baker, G., Race, P., Adams, J. (2017). Studies of recombinant TWA1 reveal constitutive dimerization. *Bioscience Reports, 37* (1).

Franke, D., Svergun, D. (2009). DAMMIF, a program for rapid ab-initio shape determination in small-angle scattering. *Journal of Applied Crystallography, 42* (2), 342–346.

Franke, D., Petoukhov, M., Konarev, P., Panjkovich, A., Tuukkanen, A., Mertens, H., Svergun, D. (2017). ATSAS 2.8: a comprehensive data analysis suite for small-angle scattering from macromolecular solutions. *Journal Of Applied Crystallography*, 50, 1212–1225.

Gallat, F., Brogan, A., Fichou, Y., McGrath, N., Moulin, M., Perriman, A. (2012). A Polymer Surfactant Corona Dynamically Replaces Water in Solvent- Free

Protein Liquids and Ensures Macromolecular Flexibility and Activity. *Journal of the American Chemical Society*, *134* (32), 13168−13171.

Goodfellow, M., Stach, J., Brown, R., Bonda, A., Jones, A., Mexson, J., Bull, A. (2012). Verrucosispora maris sp. nov., a novel deep-sea actinomycete isolated from a marine sediment which produces abyssomicins. *Antonie van Leeuwenhoek, 101* (1), 185-193.

Hashimoto, T., Kuzuyama, T. (2016). Mechanistic insights into Diels-Alder reactions in natural product biosynthesis. *Current Opinion in Chemical Biology*, 35, 117-123.

Hermanson, G. (1996). Bioconjugate techniques. *Academic Press, 40* (4), 631–631.

Hermanson, G. (2013). PEGylation and Synthetic Polymer Modification. *Bioconjugate Techniques*. London: Elsevier Inc, 787-838.

Horie, M., Fujita, K. (2011). Toxicity of Metal Oxides Nanoparticles. *Advances in Molecular Toxicology*, 1048, 99–122.

Hughes, D., Karlén, A. (2014). Discovery and preclinical development of new antibiotics. *Upsala Journal Of Medical Sciences, 119* (2), 162–169.

Hura, G., Menon, A., Hammel, M., Rambo, R., Poole, F. (2009). Robust, high-throughput solution structural analyses by small angle X-ray scattering (SAXS). *Nature Methods, 6*, 606–612.

Kleckner, I., Foster, M. (2011). An introduction to NMR-based approaches for measuring protein dynamics. *Biochimica et Biophysica Acta, 1814* (8), 942–968.

Konarev, P., Volkov, V., Sokolova, A., Koch, M., Svergun, D. (2003). PRIMUS: a Windows PC-based system for small-angle scattering data analysis. *Journal of Applied Crystallography, 36* (2), 1277–1282.

Lawrence, M., Phillips, K., Liu, D. (2007). Supercharging Proteins Can Impart Unusual Resilience. *Journal Of The American Chemical Society, 129* (33), 10110–10112.

Lipshutz, B., Ghorai, S. (2014). Transitioning organic synthesis from organic solvents to water. What's your E Factor? *Green Chemistry, 16* (8), 3645–4018.

Liu, Y., Hsieh, C., Chen, Y. (2006). Thermally reversible cross-linked polyamides and thermo-responsive gels by means of Diels–Alder reaction. *Polymer, 47* (8), 2581-2586.

Mant, C., Hodges, R. (2006). Context-dependent effects on the hydrophilicity/hydrophobicity of side-chains during reversed-phase high-performance liquid chromatography: Implications for prediction of peptide retention behaviour. *Journal of Chromatography A, 1125* (2), 211-219.

Montalbetti, C., Falque, V. (2005). Amide bond for- mation and peptide coupling. *Tetrahedron, 61* (8), 10827–10852.

Nozue, Y., Shinohara, Y., Amemiya, Y. (2007). Application of Microbeam Small- and Wide-angle X-ray Scattering to Polymeric Material Characterization. *Polymer Journal, 39*, 1221–1237. Retrieved January 30, 2018, from Polymer Journal [online]. Available at: http://main.spsj.or.jp/c5/pj/pj07/pj3912.html

Osswald, C., Zipf, G., Schmidt, G., Maier, J., Bernauer, H., Müller, R., Wenzel, S. (2014). Modular construction of a functional artificial epothilone polyketide pathway. *ACS Synthetic Biology, 3* (10), 759-772.

Perriman, A., Cölfen, H., Hughes, R., Barrie, C., & Mann, S. (2009). Solvent-Free Protein Liquids and Liquid Crystals. *Angewandte Chemie*, 6242-6246.

Petoukhov, M. V. (2012). *Journal of Applied Crystallography, 45* (2), 342-350.

Preiswerk, N., Beck, T., Schulz, J., Milovnı´k, P., Mayer, C., Siegel, J., Hilvert, D. (2014). Impact of scaffold rigidity on the design and evolution of an artificial Diels-Alderase. *PNAS, 111*, 8013–8018.

Renata, H., Wang, J., Arnold, F. (2015). Expanding the Enzyme Universe: Accessing Non-Natural Reactions by Mechanism-Guided Directed Evolution. *Angewandte Chemie, 9* (54), 3351–3367.

Riedlinger, J., Reicke, A., Zähner, H., Krismer, B., Bull, A., Maldonado, L., Fiedler, H. (2004). Abyssomicins, inhibitors of the para-aminobenzoic acid pathway produced by the marine Verrucosispora strain AB-18-0. *The Journal of Antibiotics, 57*, 271–279.

Ruiz, B., Chávez, A., Forero, A., García-Huante, Y., Romero, A., Sánchez, M., Langley, E. (2010). Production of microbial secondary metabolites: regulation by the carbon source. *Critical Review Microbiology, 36* (2), 146-167.

Schmidt, N., Eger, E., Kroutil, W. (2016). Building Bridges: Biocatalytic C–C-Bond Formation toward Multifunctional Products. *ACS Catalysis, 6* (7), 4286–4311.

SMAC, U. S. (1998). *The Path of Least Resistance.* London: Department of Health.

Snider, B., Zou, Y. (2005). Synthesis of the carbocyclic skeleton of Abyssomicins C and D. *Organic Letters , 7* (22), 4939–4941.

Spicer, C., Davis, B. (2014). Selective chemical protein modification. *Nature Communications*, *1* (5).

Stanford. (2017). *Initial Analysis and Quality Assessment of Solution Scattering Data*. Retrieved February 22, 2018, from [online]. Available at: https://www-ssrl.slac.stanford.edu/~saxs/analysis/assessment.htm

Strickler, S., Gribenko, A., Keiffer, T., Tomlinson, J., Reihle, T., Loladze, V., Makhatadze, G. (2006). Protein stability and surface electrostatics: a charged relationship. *Biochemistry, 5*(9), 2761–2766.

Subramani, R., Aalbersberg, W. (2012). Marine actinomycetes: An ongoing source of novel bioactive metabolites. *Microbiological Research, 167* (10), 571-580.

Svergun, D. (1992). Determination of the regularization parameter in indirect-transform methods using perceptual criteria. *Journal of Applied Crystallography , 25*, 495–503.

Truppo, M. (2017). Biocatalysis in the Pharmaceutical Industry: The Need for Speed. *ACS Medicinal Chemistry Letters, 8* (5), 476–480.

Tung, C., C, W., Fung, E., Li, X. (2016). raceless and Chemoselective Amine Bioconjugation via Phthalimidine Formation in Native Protein Modification. *Organic Letters, 18* (10), 2600–2603.

Turner, N., Truppo, M. (2013). Biocatalysis enters a new era. *Current Opinion in Chemical Biology* (17), 212−214.

Vieweg, L., Reichau, S., Schober, R. P., & Süssmuth, R. (2014). Recent advances in the field of bioactive tetronates. *Natural Product Reports, 31*, 1554–1584.

Vieweg, L., Reichau, S., Schobert, R., Leadlay, P., Süssmuth, R. (2014). Recent advances in the field of bioactive tetronates. *Natural Product Reports* (11), 1554–1584.

Warhi, T., Al-Hazimi, H. E.-F. (2012). Recent development in peptide coupling reagents. *Journal of Saudi Chemical Society, 16* (2), 97–116.

Zalipsky, S. (1995). Functionalized poly(ethylene glycol) for preparation of biologically relevant conjugates. *Bioconjugation Chemistry, 6*(2), 150-165.

Zheng, Q., Guo, Y., Yang, L., Zhao, Z., Wu, Z., Zhang, H., Yang, H. (2016). Enzyme-Dependent [4 + 2] Cycloaddition Depends on Lid-like Interaction of the N-Terminal Sequence with the Catalytic Core in PyrI4. *Cell Chemical Biology, 23*, 352–360.